Appendix D—Compilation of Creep Rate Data for California Faults and Calculation of Moment Reduction Due to Creep

By Ray J. Weldon, II,[1] David A. Schmidt,[2] Lauren J. Austin,[1] Elise M. Weldon,[1] and Timothy E. Dawson[3]

Introduction

This appendix documents observations of creep on California faults and develops a methodology to estimate seismic moment reduction over the entire fault surface due to interseismic creep. The data presented here are an update of data originally compiled for appendix P of the Uniform California Earthquake Rupture Forecast, version 2 (UCERF2; Wisely and others, 2007). Updated time-series data developed from conventional methods, such as short baseline alignment arrays, yield results that are similar to those in UCERF2, although their precision and coverage has improved slightly with time. New geodetic estimates, particularly derived from interferometric synthetic aperture radar (InSAR), have greatly increased the density and coverage provided by conventional techniques, approximately doubling the dataset. Where the two datasets overlap, there is excellent agreement, so all data were combined to estimate along-fault average surface creep rates. Because a single value of surface creep rate is assigned to a fault "minisection" in the UCERF model that can span kilometers to tens of kilometers in length, we smoothed the raw data along strike for each fault and assigned a value for each minisection that is about the average of the smoothed rate over the section, with outliers removed. Some of the outliers are bad data points, such as low negative rates produced by InSAR in some areas, but other outliers are real spikes (high or low) in creep rate with a resolution that cannot be measured at the scale of our model, so our model necessarily removes isolated highs and lows in creep rate and varies smoothly from minisection to minisection.

In UCERF2, following the lead of previous working groups and the U.S. Geological Survey National Seismic Hazard Map (USGS NSHMP) precedent, the seismic moment generated by earthquakes from a fault section was reduced by the ratio of surface creep rate to the total fault slip rate for each fault section. For example, if the surface creep rate was one-half the fault slip rate, then the seismic moment was reduced by one-half. Fault theory and a growing body of geodetic and seismologic evidence suggests that creep at the surface generally decreases in rate with depth, so the seismic moment released by earthquakes on partially creeping faults almost certainly is systematically underestimated in UCERF2 and similar previous models. In appendix D, we develop and apply an alternative approach to estimating how creep is extrapolated to the entire fault plane from surface observations, and estimate moment reduction

[1]University of Oregon.
[2]University of Washington.
[3]California Geological Survey.

for fault sections using only the surface creep rate and total fault slip rate. In reality, how creep varies with depth almost certainly differs between faults and probably even along strike for individual faults; however, for a uniform model that spans all of California, we need a simple approach that shows the general behavior of all faults. Our new model is simple enough to apply uniformly, improves on the UCERF2 approach, and is consistent with the available data and our current (2013) state of knowledge.

Background

Observation of creep on faults is a critical part of our earthquake rupture model because the moment released as earthquakes is reduced, from what would be inferred directly from the fault's slip rate, if a fault is observed to creep. There is considerable debate about the extent to which creep (measured at the surface during a short time period) represents the whole fault surface through the entire seismic cycle (for example, Hudnut and Clark, 1989; Wei and others, 2009), and observationally, it is clear that the amount of creep varies spatially and temporally on a fault (for example, Schmidt and others, 2005; Shirzaei and Burgmann, 2013). However, from a practical point of view, a single creep rate needs to be associated with a fault section (or whatever discretization of a fault is selected for the model) and the reduction in seismic moment generated by the fault is accommodated in a seismic hazard model by reducing the surface area that generates earthquakes or by reducing the slip rate on the fault that is converted to seismic energy. UCERF2 followed the practice of past working groups and the USGS NSHMP, and used creep rate (where it was judged to be interseismic) to reduce the area of the fault surface that generates seismic events. In addition to following past practice, this decision allowed the working group to use a reduction of slip rate as a separate factor to accommodate aftershocks, post-seismic slip, possible aseismic permanent deformation along fault zones, and other processes that are inferred to affect the entire surface area of a fault, and, therefore, are better modeled as a reduction in slip rate. In UCERF2, C-zones also were handled by a reduction in slip rate because they are inferred to include regions of widely distributed shear that is not completely released as earthquakes large enough to model. As discussed in the Uniform California Earthquake Rupture Forecast, version 3 (UCERF3, this report), the working group decided to adopt a hybrid approach, which is to reduce area for faults with low to moderate creep rates (relative to the fault slip rate) and to add slip rate reduction as the creep rate approaches the slip rate.

In UCERF2, the ratio of the rate of creep relative to the total slip rate was used to calculate an aseismic fraction of the fault surface, measured down from the surface, so this depth reduced the surface area of a fault that generates earthquakes in the model, reducing its seismic moment release. This reduction of surface area of rupture was described by an aseismicity factor, assigned to each creeping fault in appendix A of UCERF2 (Wills and others, 2007). An aseismicity factor of less than 1 is only assigned to faults that are inferred to creep during the entire interseismic period. For each section of a fault that creeps, a single aseismicity factor was assigned by expert opinion based on the observations in the UCERF2 database. Uncertainties were not determined for the aseismicity factor, and it, therefore, represented an unmodeled (and difficult to model) source of error. Based on UCERF3 observations and understanding of how faults creep, the UCERF2 approach (which essentially was the approach used by all previous working groups) overestimates the reduction of moment in earthquakes because it does not take into account the now generally accepted fact that creep is shallow and decreases rapidly in rate with depth. Our approach for UCERF3 accounts for creep rate reduction with depth, and, therefore, is a significant improvement over UCERF2, although it probably only shows the average behavior of creeping faults that almost certainly vary considerably in individual behavior.

Creep Observations

Surface creep commonly refers to relatively aseismic fault slip occurring at or near the surface (Wesson, 1988); while creep is usually accompanied by small earthquakes, it is referred to as "aseismic" because few large earthquakes occur and the rate of surface slip associated with the creep is much greater than would be inferred from the associated microseismicity. Evidence for surface creep is well documented along the San Andreas Fault system (figs. D1 and D2). It is not known if creep is limited to the major strike slip faults or if these faults slip more rapidly so the creep is evident. Additionally, the San Andreas Fault zone has been more intensively surveyed for creep compared to other faults. Because creep usually is only a fraction of a fault's slip rate, it would be difficult to recognize creep on most California faults that have slip rates of about 1 mm/yr or less.

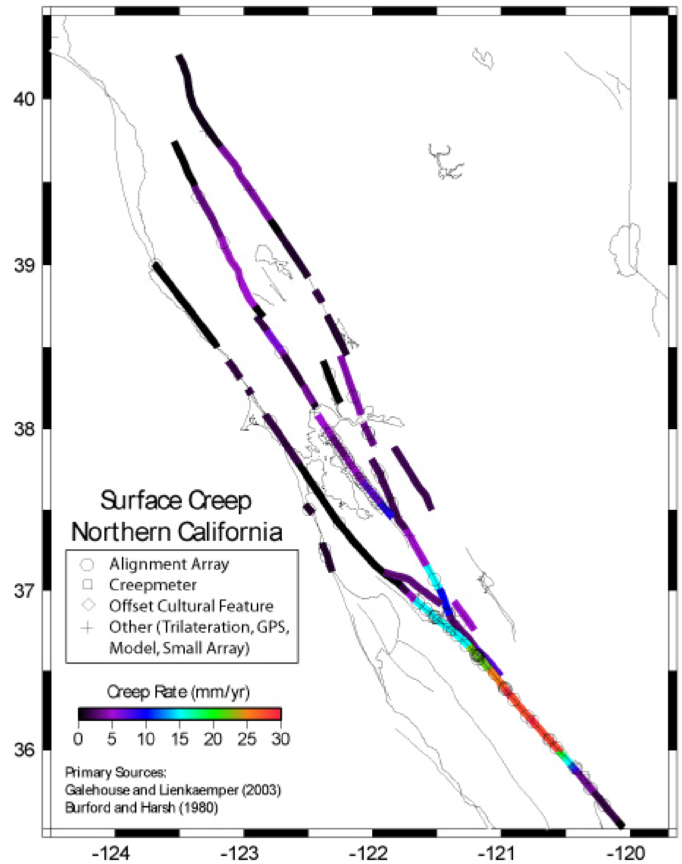

Figure D1. Map showing creep rates of northern California faults (figure updated from appendix P of Uniform California Earthquake Rupture Forecast, version 2; Wisely and others, 2007). Heavy black lines indicate documented absence of creep; that is, places where attempts have been made to identify creep so creep can be limited to a small fraction of the fault's slip rate. Gaps in black lines in faults along the coast are offshore minisections where creep cannot be measured, but where creep rates are likely to be zero like in adjacent onshore minisections. Small (faint) symbols indicate the locations of creep observations that are summarized in table D2.

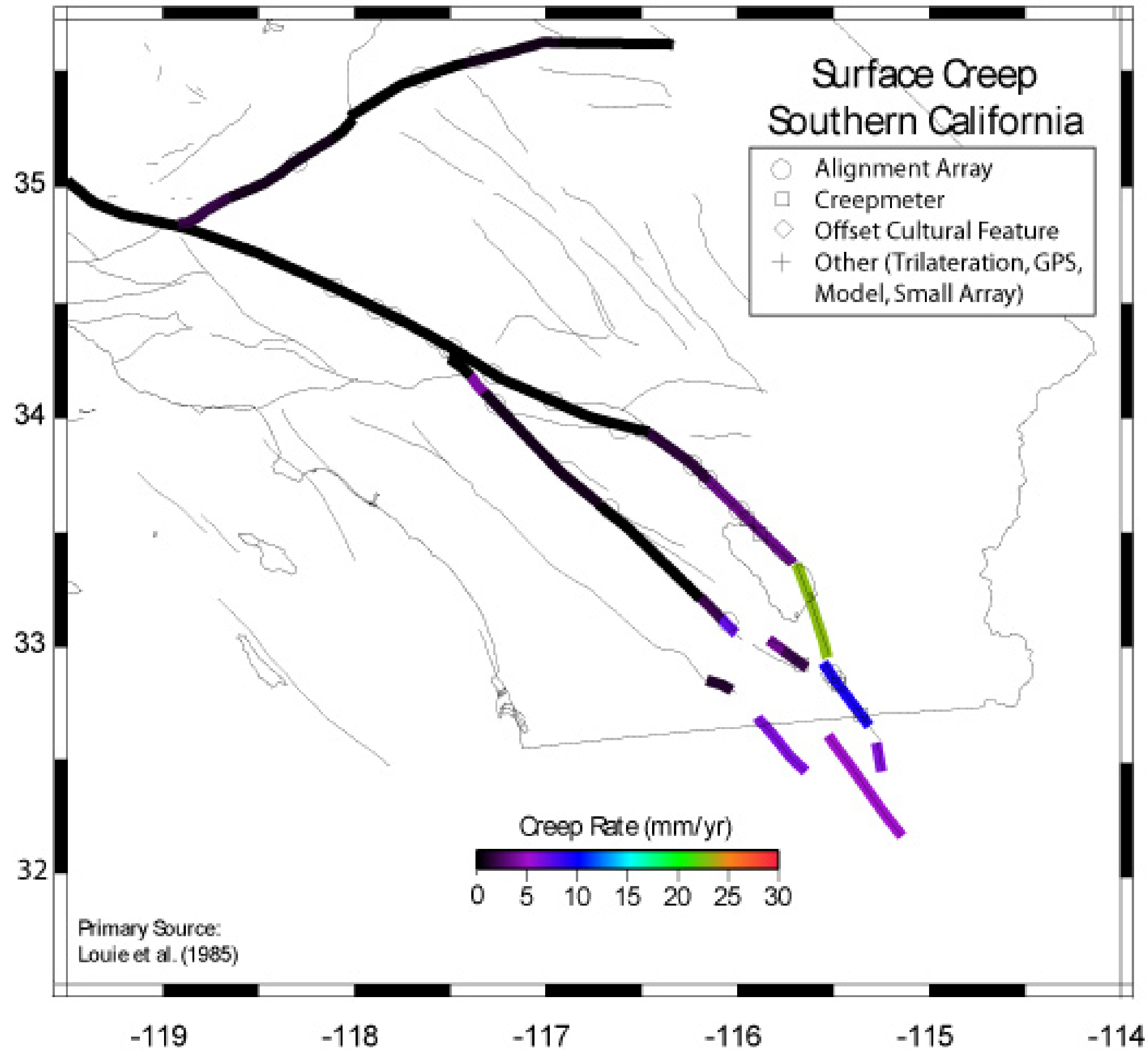

Figure D2. Map showing creep rates of southern California faults (figure updated from appendix P of Uniform California Earthquake Rupture Forecast, version 2; Wisely and others, 2007). Heavy black lines indicate documented absence of creep; that is, places where attempts have been made to identify creep and it can be limited to a small fraction of the fault's slip rate. Small (faint) symbols indicate the locations of creep observations that are summarized in table D2.

Fault creep can be continuous in time or consist of a series of steps (creep events; see fig. D3 for an example). Creep that persists for several decades often is referred to as “interseismic creep” and is inferred to span the entire time between large seismic events. Accelerated surface slip also can be observed following a major earthquake, in which case it is referred to as “afterslip.” Short-term fluctuations in creep rate that deviate from long-term rates for weeks or months can be referred to as “transient creep” or “triggered creep” in the case where a localized stress perturbation is imposed (Burford, 1988). Few of our observations include obvious afterslip from a significant local earthquake, but all include small triggered events. From a practical point of view, we do not attempt to distinguish triggered creep from creep that is not obviously associated with an event; we calculate creep rate by using the beginning and end of the available times series.

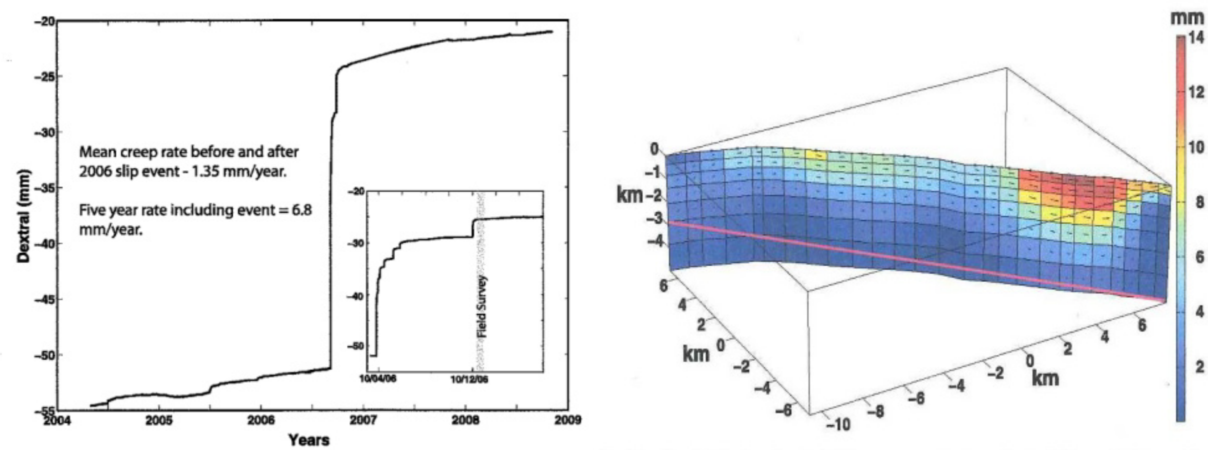

Figure D3. Creep consists of both long term, often steady, slip and incremental slip events associated with or triggered by earthquakes or strain events. Example above, from Wei and others, 2009, shows (left, Figure 2 in Wei and others, 2009) how steady creep of 1.35 mm/yr occurs before and after an abrupt creep event of 27 mm in October of 2006. A 5-year average rate from 2004 to 2009 yields a rate of 6.8 mm/yr, illustrating that the rate is dominated by the frequency of creep events. Modeling of this event (right, Figure 8 in Wei and others, 2009) suggests that the abrupt creep event was very shallow, extending only to 3 or 4 km at its deepest point. All of our creep rates include both steady creep and discrete events like this; for the purpose of UCERF3 we simply calculate the creep rate from the beginning to the end of each available time series.

In addition to updating the creep rates determined from traditional ground-based observations, we have added a significant new data source, based largely on InSAR (fig. D4; table D2). Although many workers have determined creep from geodetic techniques, we have adopted the results of Tong and others (2013) as the most complete dataset that extends the length of the San Andreas Fault system. These Advanced Land Observing Satellite L-band results span a very short time period and do not easily resolve low rates of creep; however, these results represent a completely independent set of observations that generally agree well with traditional land-based techniques and greatly expand coverage, providing a more complete picture of the rapidly creeping faults (fig. D4).

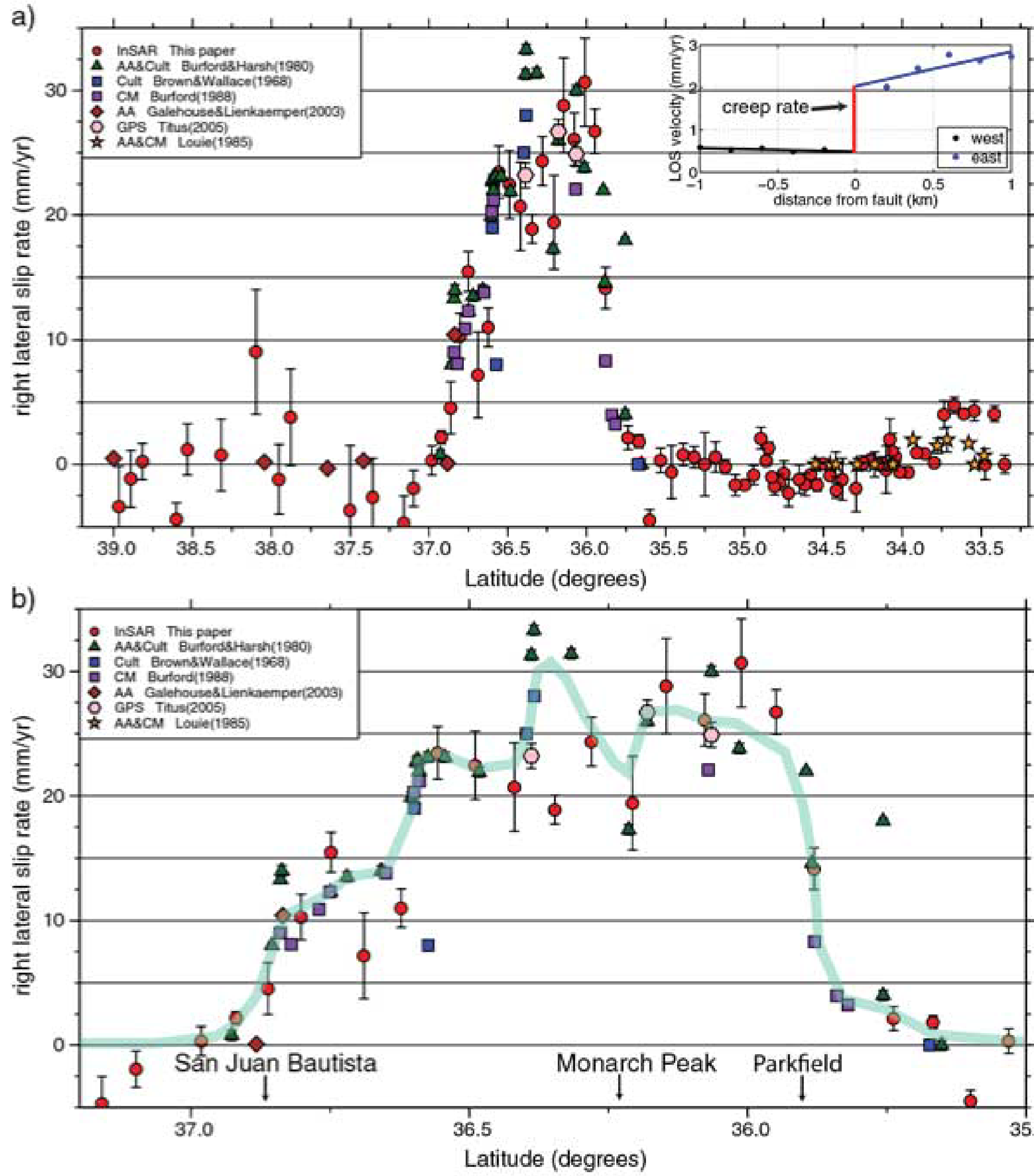

Figure D4. Graphs showing example of creep data profile along the San Andreas Fault, California (figure modified from Tong and others, 2013). There is good agreement between different measurement techniques. Interferometric synthetic aperture radar (InSAR) has dramatically increased the number of measurements since Uniform California Earthquake Rupture Forecast, version 2 (UCERF2), although results in some areas still have considerable scatter owing to the short time scale and limited number of epochs of observations. The aqua line in the lower figure (b) is a hand-drawn smooth fit to the data that illustrates how the data were smoothed to estimate the average creep rates for each minisection in the Uniform California Earthquake Rupture Forecast, version 3 (UCERF3) model (table D1). Similar smooth curves were drawn for each fault, and average creep rates for each UCERF3 minisection were estimated. Non-InSAR data are essentially the UCERF2 compilation, which was built from slightly different references, cited therein, and updated in UCERF3.

Because the creep data are not spatially uniform and because we need a single value to apply to each element of the UCERF model, we drew smooth curves through the surface creep data, ignoring outlier points (see fig. D4*b* for an example on the San Andreas Fault). We then assigned a value for each minisection (table D1), which can span kilometers to tens of kilometers in length that is approximately the average of the smoothed rate across the section. Some of the outliers are bad data points, such as low negative rates produced by InSAR in some areas, but other outliers are real spikes (high or low) in creep rate with a resolution that cannot be measured at the scale of our model, so our model necessarily removes isolated highs and lows in creep rate and varies smoothly from minisection to minisection. Because each deformation model has a fault slip rate assigned to each minisection, we can determine the ratio of surface creep rate to total fault slip rate for all minisections that creep. This ratio, called the "aseismicity factor," will be the basis for determining the percentage of seismic moment reduction owing to creep for that part of the fault.

How Creep Varies with Depth

Because creep rate varies with depth and generally is observed directly only at the surface, a model is needed to describe, at least on average or in theory, how creep rate changes with depth. Most theory (for example, Savage and Lisowski, 1993) and a growing body of observations (Sieh and Williams, 1990 Manaker and others*,* 2003; figs. D5 and D6 of this report) suggest that for moderately to relatively slowly creeping faults, creep rate decreases rapidly with depth. The two places with the best resolution of how creep rate varies with depth are along the San Andreas Fault near Parkfield, California, and along the Hayward Fault in the San Francisco Bay Area. Near Parkfield, the surface creep rate diminishes from approximately 25 to 0 mm/yr over about a 40-km stretch of the fault (fig. D4). The overall fault geometry is simple, without junctions or other nearby faults, so it is almost certain that at depth, below the seismogenic zone, the slip rate is constant through this stretch of the San Andreas Fault. The Parkfield region is densely instrumented with Global Positioning System (GPS) sites and other instruments for measuring surface deformation, so it is possible to invert for slip rate at depth along the fault (fig. D5; Murray and others*,* 2001). Creep rate decreases rapidly with depth, reaching a minimum in the middle part of the seismogenic zone, at a depth of about 5–8 km. Murray and others (2001) inversion also suggests an increase in slip rate with depth through the lower part of the seismogenic zone as the transition depth (where the full slip rate occurs) is approached.

The second place where a dense dataset of observations allows inferences of how creep decreases with depth is along the central Hayward Fault. Savage and Lisowski (1993) have modeled how creep decreases with depth and recent inversion of geodetic data allows an image of how creep varies with depth and along strike. We adopt the method of Savage and Lisowski (1993) to calculate profiles of creep rate with surface creep at rates of up to 50 percent of the slip rate (see fig. D9 for the Hayward Fault). At the other end of the creep rate spectrum, it is widely believed that when the surface creep rate equals the fault slip rate, the entire fault surface is creeping at the slip rate and, therefore, no elastic strain (that could be released as seismic moment) accumulates. Although we do not consider this to be established fact, we assume this is the case for our model. For faults that creep at rates of between 50 and 100 percent of their slip rate, we assume that the distribution of creep rate smoothly transitions from the Savage and Lisowski (1993) 50-percent model to fully creeping on the entire fault plane, as shown in figure D9.

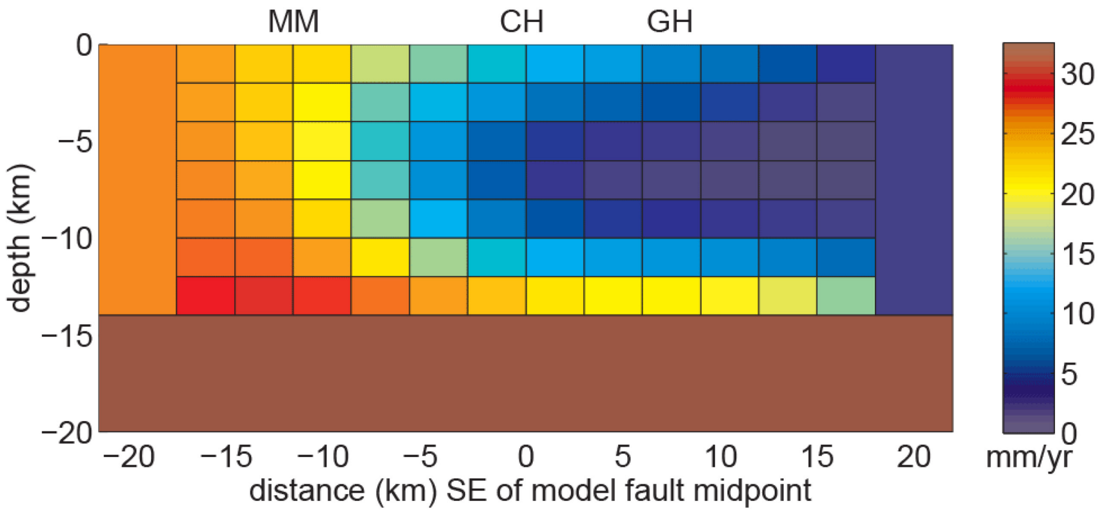

Figure D5. Graph showing interseismic creep rate as a function of depth (from Murray and others, 2001) for the Parkfield, California, part of the San Andreas Fault (Parkfield is at 0 kilometers). Blocks are uniformly slipping dislocations in the region between the Creeping Section (left) to the fully locked southern San Andreas Fault to the south (right). The slip rate in the Creeping Section is assumed to be 24 millimeters per year and calculated at 33 millimeters per year below the transition zone at a depth of 14 kilometers. In the center of the model, where the resolution is best, the slip rate at the surface (measured creep) decreases with depth down to a minimum rate at 5–8 kilometers, and then the creep rate increases down to the transition zone.

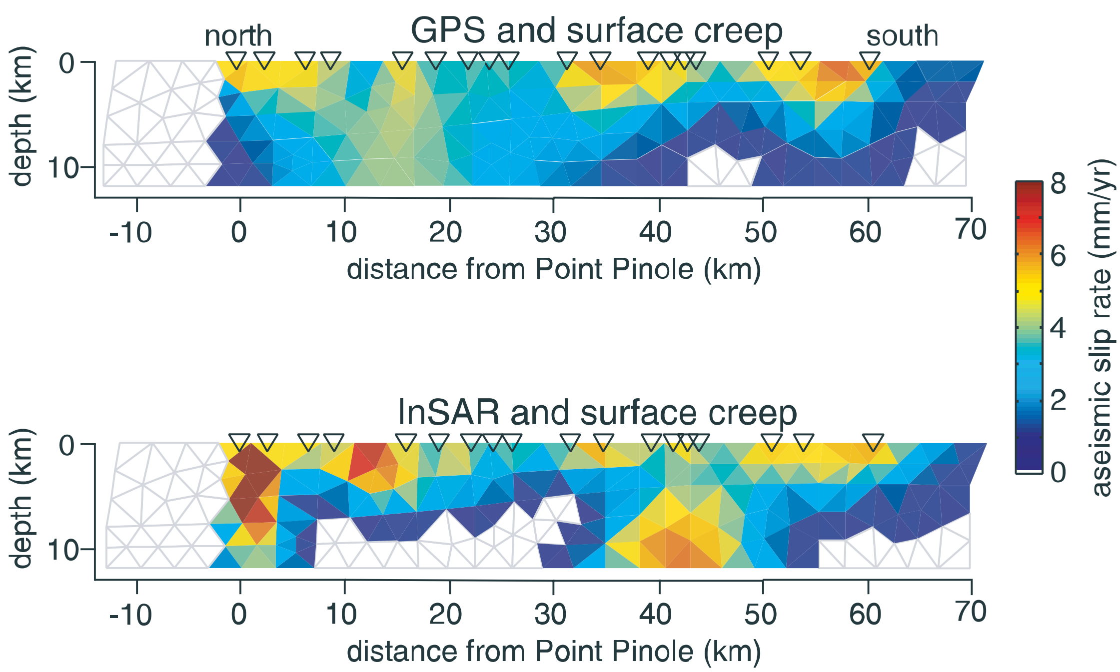

Figure D6. Graphs showing an example (from Schmidt and others, 2005) suggesting that the Hayward Fault, which creeps at about one-half of its slip rate, creeps down to about one-half of its widely accepted locking depth. A growing dataset of dense geodetic observations suggest that, in most cases, creep is shallow relative to the locking depth of seismogenic faults.

Another possible approach to determining how creep varies with depth is to examine small, repeating earthquakes (REs) that are inferred to sample the interseismic slip rate of the fault in which their sources are embedded (for example, Templeton and others, 2008). The most complete dataset exists along about a 30-km stretch of the San Andreas Fault near San Juan Bautista (36.64–36.83 degrees N). Over this stretch of the San Andreas Fault, the surface creep rate increases from about 10 to 20 mm/yr, so we can compare slip rates at depth inferred from the small REs to those measured at the surface. Superficially, the southern half of this stretch of the fault shows some agreement with the theory we apply here; figure D7 (fig. S6 in Templeton and others, 2008) shows a decrease in slip rate (in this figure, total RE slip during an interval of time) with depth, and figure D8 (figure S8 in Templeton and others, 2008) shows an increase in depth of creep to the south, which would be expected as the surface creep rate increases to the south. However, the northern part of this study area (figs. 7 and 8 in Templeton and others, 2008; not included here) does not obviously show this relationship (in part because there are virtually no REs at depths of less than 5 km that can be used to document the shallow creep rate), and in detail, it is difficult to document a quantitative relationship in the southern part.

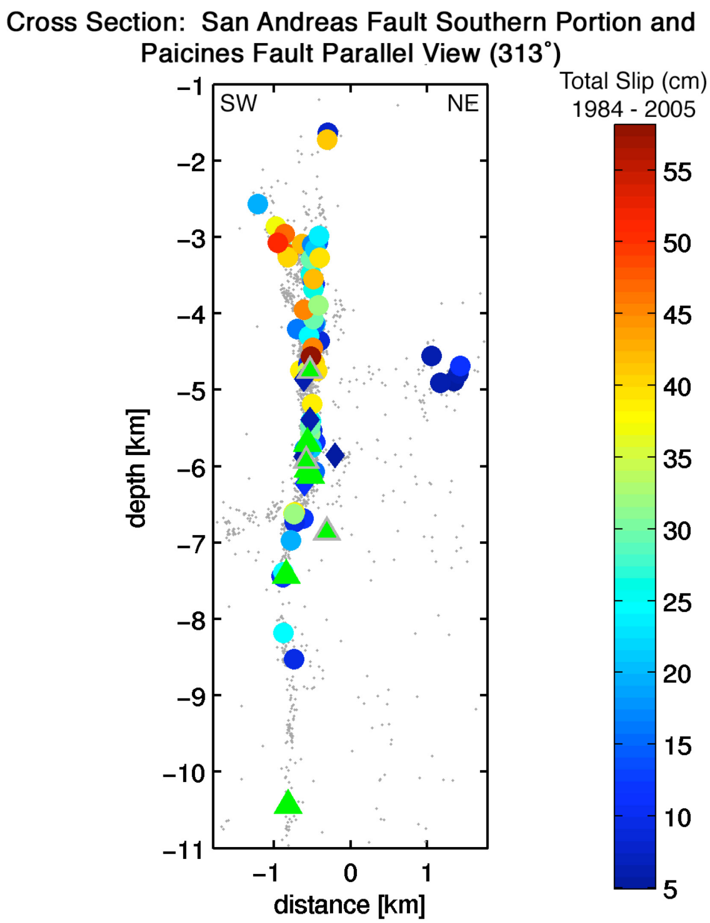

Figure D7. Cross section (parallel view) showing southern part of San Andreas Fault and Paicines Fault, California (figure S6, Templeton and others, 2008) with a decrease in slip rate (in this figure total slip of repeating earthquakes during an interval of time) with depth.

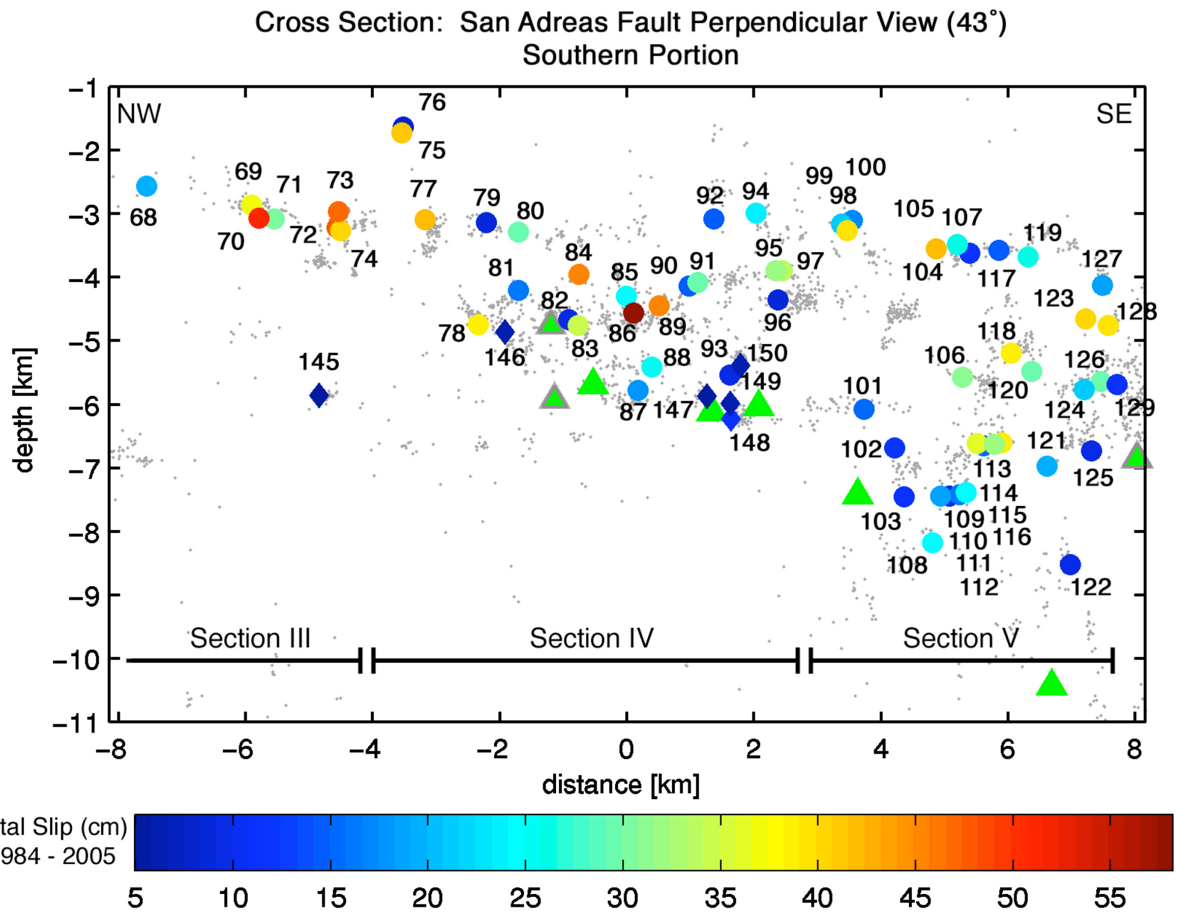

Figure D8. Cross section (perpendicular view) showing southern part of San Andreas Fault, California (figure S8 from Templeton and others, 2008) with an increase in depth of recurring earthquakes, inferred to indicate an increase in depth of creep as the surface creep rate increases from about 13 to 20 millimeters per year (left to right, northwest to southeast) across this part of the San Andreas Fault. Although generally the creep rate (here shown as total recurring earthquake slip during an interval of time) decreases with depth, there is considerable scatter in the data and apparently very different creep rates inferred from closely spaced repeating earthquakes. For this reason, we averaged creep rates across fault sections for the comparison discussed in the text.

Creep rates inferred from adjacent REs vary considerably (fig. D8); in an attempt to see a simple pattern, we averaged the creep rate across each of the five sections defined by Templeton and others (2008) to compare to the surface creep. We also calculated an inferred slip rate from their data (Templeton and others, 2008, presented their data as total slip in centimeters between 1984 and 2005, not slip rate) and included our slip rates as table D3. This was necessary because some RE sequences only had a few events, and the first and last event in the series often did not correspond to the time period 1984–2005; therefore, we divided the average slip per event by the average time between events to calculate the slip rate. This generally produced higher slip rates than those resulting from dividing by the time between 1984 and 2005 because REs do not occur exactly at the beginning and end of the time period, so we generally divided by a shorter time period.

Section (NW end lat/long)	**Ave RE depth (km)**	**Ave RE slip rate (mm/yr)**	**Surface creep rate (mm/yr)**
1 (36.8242,-121.5483)	5	14	10
2 (36.7822,-121.4809)	7	10	12
3N (36.7400,-121.4166)	7	9	13
3S (36.7329,-121.3867)	3	19	14
4 (36.7120,-121.3477)	4	12	15
5 (36.6687,-121.2870)	5	10	19

See table D3 for Templeton and others' (2008) data that contributed to these averages; see figure D4 for surface creep rates on the San Andreas Fault at the corresponding latitudes.

Across the entire stretch of the fault, the average from Templeton and others (2008) is slightly less than the surface creep average (12.3 versus 13.8 mm/yr). In the data shown in the in-text table above, there is some suggestion for a decrease in creep rate with depth; some adjacent sections show increases in average depth; for example, section 2 is deeper than 1 and creeps more slowly; sections 3S to 3N and 4 to 5 have lower rates with depth, although 3S to 4 does not follow this pattern. Additionally, the observed progressive increase in surface creep rate from 10 mm/yr in the north (section 1) to 19 mm/yr in the south (section 5) is not obvious in the data from Templeton and others (2008), and the RE creep rates for sections 1 and 3S almost certainly are higher than the surface rates. Similarly, RE-inferred creep rates on other minor faults discussed by Templeton and others (2008), such as the Quien Sabe (up to 12 mm/yr), are almost certainly an order of magnitude greater than the respective long-term slip rates of those faults.

The very high rates inferred from the fastest-slipping individual RE sequences on the San Andreas Fault, up to five times greater than the total fault slip rate. The fact that the average of some sections exceeds the surface creep rate, suggest that the RE approach may systematically overestimate creep rate or may represent a short acceleration of creep, perhaps triggered by nearby large earthquakes. The possibility of an overestimated creep rate is suggested by Templeton and others (2008), and the short acceleration of creep may result from how the RE rates are calibrated. The RE creep rate was calibrated near Parkfield using the surface creep rate (Nadeau and McEvilly, 1999, 2004; Nadeau, 2007) above RE sequences. If creep decreases with depth, as is widely believed regionally and shown by Murray and others (2001) at Parkfield, slip rates from RE sequences systematically are overestimated in terms of how they have been calibrated.

In summary, a review of the Templeton and other*,* (2008) dataset supports a decrease in creep rate with depth and an increase in the depth of creep with increased creep rate, as theory suggests. However, a much more careful comparison of REs and surface creep rates would be required to quantify this relationship.

Moment Reduction

In UCERF2, following the lead of previous working groups and the USGS NSHMP precedent, the seismic moment generated by a fault section was reduced by the ratio of surface creep rate to the total fault slip rate for each fault section. For example, if the surface creep rate were one-half the fault slip rate, the seismic moment released by earthquakes was reduced by one-half. This is incorrect if creep decreases with depth, as we have shown. However, there is no generally accepted quantitative theory for how creep rate decreases with depth and, therefore, for how to calculate the resulting moment reduction. We used the approach of Savage and Lisowski

(1993) in this study for creep rates of up to 50 percent of the slip rate, and conceptually extended it (fig. D9).

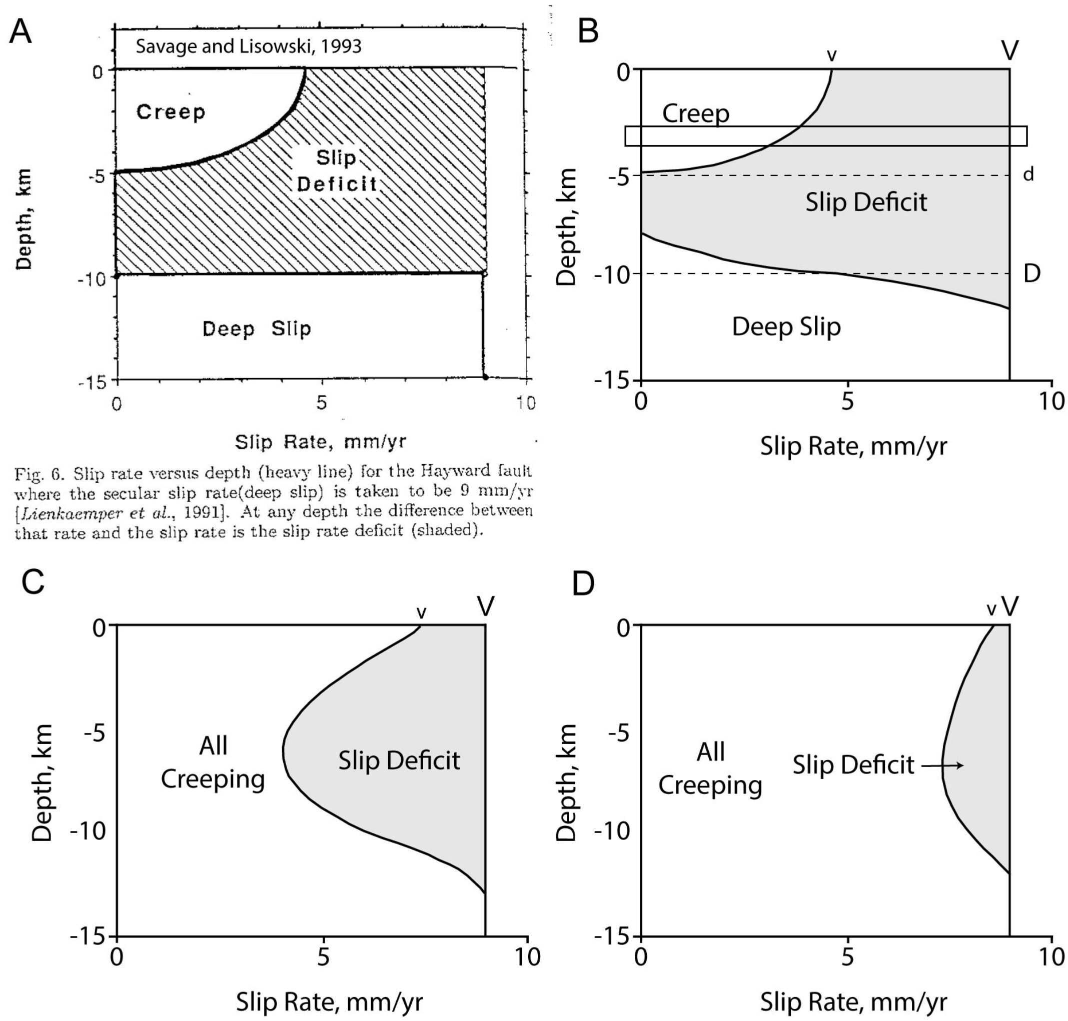

Figure D9. Plots showing variation of slip rate with depth for the Hayward Fault. For creep rates of less than one-half the fault slip rate, we used the formulation of Savage and Lisowski, 1993 (panel A), modified slightly to include a “transition” zone at the base of the locked part of the fault (panel B); this modification does not change the amount of moment released in earthquakes by the fault because it has the same average depth (D) of the abrupt boundary in the Savage and Lisowski (1993) model and, therefore, the same slip deficit. For a surface creep rate (v) of about one-half the slip rate (V), creep depth (d) is about one-half the locking depth (D), and the creep rate decreases asymptotically to 0 at d. Geodetic models such as those shown in figures D5 and D6 suggest that as creep rate (v) approaches the slip rate (V), the creep rate at depth approaches the creep rate at the surface, creating profiles such as shown in panels C and D. Although the exact shape of the depth profile in panel C is poorly known from theory and observation, we progressively evolved its shape from that in panel B into a flat vertical profile in which creep rate equals slip rate slip at all depths. Narrow horizontal box in panel B shows how moment is calculated in 1-kilometer strips, as discussed in the text.

Figure D9*A* is figure 6 of Savage and Lisowski (1993), and figure D9*B* modifies it slightly with a tapered transition zone. “V” is the fault slip rate (in this case, 9 mm/yr), and “v” is the creep rate (in this case, 4.5 mm/yr at the surface and decreasing to 0 mm/yr at a depth of 5 km). The “slip deficit” is the fault slip rate, V, minus the creep rate, v (at any given depth) integrated over the surface area of the fault. If a fault does not creep, the slip deficit is the slip rate, and the seismic moment that the fault accumulates is μ*fault area*slip rate. Assuming a unit of fault length, a fault area can be thought of conceptually as depth. If the fault creeps we could still calculate the seismic moment the fault is accumulating by thinking of the fault plane as a stack of 1-km strips (such as that shown in fig. D9*B* for a depth of 3–4 km). We calculate the moment for each 1-km strip as μ*1 km of fault depth*slip deficit rate (V-v for that 1 km strip), and sum all the 1-km strips to get the total seismic moment accumulation.

Potential seismic moment is accumulating not just across the fully locked part of the fault surface, but also across the creeping parts because the creeping fault surface slips at less than the full slip rate. We can then compare this creep-reduced seismic moment to that expected for a fully locked fault and express the result as a simple ratio (fig. D10); in this example we get about 20-percent less moment for a fault that creeps at about one-half of its slip rate.

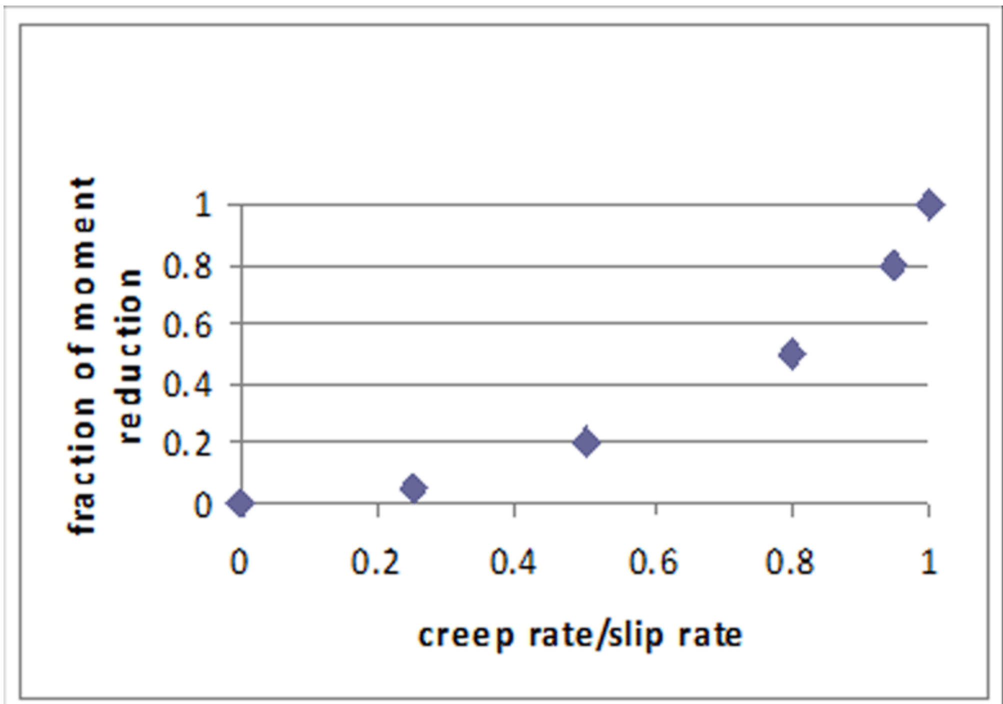

Figure D10. Graph showing moment reduction using the model in figure D9 to calculate slip rate as a function of depth given creep rate, fault slip rate and a fault depth of about12 kilometers. We can calculate moment (μ*area*effective slip rate) by integrating with depth the slip rate versus depth profile shown in figure D9. Because μ also is a constant (elasticity constant), we can use this relationship to reduce the seismic moment if we reduce the area and hold the slip rate constant, or to reduce the seismic moment by reducing the average slip rate if we hold the fault surface area constant.

The relationships presented by Savage and Lisowski (1993), which allow us to calculate creep rate (v) as a function of depth, cannot be applied beyond about the 50-percent-of-slip-rate level shown here. As shown in figures D5 and D6, the transition zone likely rises up as creep extends deeper and deeper, as shown in figure D9*B*. Eventually, there is no part of the fault zone that is fully locked, and the creep rate decreases down from the surface and up from the transition zone. As the fault becomes completely unlocked and the creep rate approaches the slip rate, it seems reasonable that there is no slip deficit anywhere on the fault plane. We, therefore, progressively smoothed the slip deficit between the likely situation in figure D9*B* to figure D9*C* and finally to figure D9*D*. We kept the peak in slip deficit between 5 and 8 km, as suggested by the Parkfield inversion (fig. D5), and proportionately reduced its magnitude as the creep rate approached the slip rate, so the profile is completely flat with 100-percent creep.

To construct our moment reduction curve (fig. D10), we assumed that there is no moment reduction for a fully locked fault, and 100 percent moment reduction for a fault that creeps at its slip rate. For creep rate to slip rate fractions of 25 and 50 percent, we used the relationships in Savage and Lisowski (1993) to determine creep rate decrease with depth (50-percent case shown in fig. D9) and, for fractions of 80 and 95 percent, we integrated (in 1-km strips) our smoothly extrapolated creep versus depth profiles shown as figures D9*C* and D9*D*.

Because our model smoothly varies, the relationship between creep rate and slip rate and moment reduction (expressed as a fraction) varies as well. For the current version of the UCERF3 model, we extrapolated between points on figure D10 to determine the moment reduction for each creeping minisection, using its ratio of surface creep (table D1) to slip rate for each deformation model. For now, we have ignored complications, such as varying locking depths, different stressing rates on faults, and so on to generate a model that could be applied easily to all our creeping faults using their creep and slip rates. Although these factors are undoubtedly important and our model is unlikely to match any specific fault, which likely has its unique heterogeneities, this model is substantially more accurate than previous models, because it attempts to account for changes in rate as a function of depth.

Finally, as noted in the caption for figure D10, the approach of our model can be used to reduce area or slip rate in a seismic hazard model. Because moment is μ*area*effective slip rate, if either the fault area or slip rate is held constant, a linear relationship exists between moment and the remaining parameter that varies, so the approach outlined can be applied to either a reduction in area or slip rate. For UCERF3, we generally reduce the upper fault area for faults with low to moderate creep rates (relative to fault slip rate). This makes sense because most of the moment reduction owing to creep is believed to be shallow (fig. D9), and using the moment reduction factor, we reduce the “effective” fault surface by the appropriate amount. For high creep rate faults, essentially the entire fault surface is creeping (fig. D9), so reducing slip rate over the entire fault surface as well is consistent with the approach we have adopted here.

Acknowledgments

We greatly appreciate reviews by Roland Burgmann, Wayne Thatcher, Bob Simpson, and Yuri Fialko, and discussion with many members of the UCERF3 team, especially Glenn Biasi, Ned Field, and Morgan Page. We thank Xiaopeng Tong and Dave Sandwell for sharing their InSAR data well in advance of publication and the reproduction of their figure 17 (Tong and others [2013]), Jim Lienkaemper for directing us toward new ground-based data, Kevin Milner for technical assistance, and Beth Wisely for early updates to the original UCERF2 compilation.

This project was supported in part by Southern California Earthquake Center grants 157576 and 119939.

Selected References

Agnew, D.C., and Wyatt, F.K., 2010, Continuous broadband monitoring of crustal deformation near active faults in southern California: U.S. Geological Survey NEHRP Final technical report no. 07HQAG0025, May 31, 2010.

Bilham, R., Suszek, N., and Pinkney, S., 2004, California creepmeters: Seismological Research Letters, v. 75, no. 4, p 481–492.

Brown, R.D., Jr., and Wallace, R.E., 1968, Current and historic fault movement along the San Andreas Fault between Paicines and Camp Dix, California, *in* Grantz, A., and Dickinson, W.R., eds., Proceedings, Conference on geologic problems of the San Andreas Fault system: Stanford University Publications in Geological Sciences, v. 11, p. 22–39.

Burford, R.O., 1988, Retardations in fault creep rates before local moderate earthquakes along the San Andreas Fault system, central California: Pure and Applied Geophysics, v. 126, p. 499–529.

Burford, R.O., and Harsh, P.W., 1980, Slip on the San Andreas Fault in central California from alignment array surveys: Bulletin of the Seismological Society of America, v. 70, no. 4, p. 1233–1261.

Freymueller, J. T., Murray, M.H., Segall, P., and Castillo, D., 1999, Kinematics of the Pacific-North America Plate Boundary Zone, northern California, Journal of Geophysical Research, v. 104, no. B4, p. 7419–7441, doi:10.1029/1998JB900118.

Galehouse, J.S., and Lienkaemper, J.J., 2003, Inferences drawn from two decades of alignment array measurements of creep on faults in the San Francisco Bay region: Bulletin of the Seismological Society of America, v. 93, p. 2415–2433.

Glowacka, E., Sarychikhina, O., Nava, F.A., Suarez, F., Ramirez, J., Guzman, M., Robles, B., Farfan, F., and De Cossio Battani, G.D., 2010, Continuous monitoring techniques of fault displacement caused by geothermal fluid extraction in the Cerro Prieto Geothermal Field (Baja California, Mexico): International Association of Hydrological Sciences-Association Internationale des Sciences Hydrologiques publication, p. 326–332.

Glowacka, E., Sarychikhina, O., Suarez, F., Nava, F., Farfan, F., Cossio Battani, G.D., and Guzman, M., 2007, Aseismic slip observed on the faults in Mexicali Valley, Baja California, Mexico [abs.]: Eos (American Geophysical Union Transactions), v. 88, no. 23, Joint Assembly Supplement, abs. G33A-04.

Goulty, N.R., Burford, R.O., Allen, C.R., Gilman, R., Johnson, C.E., and Keller, R.P., 1978, Large creep events on the Imperial Fault, California: Bulletin of the Seismological Society of America, v. 68, p. 517–521.

Harris, R.A., and Segall, P., 1987, Detection of a locked zone at depth on the Parkfield, California, segment of the San Andreas Fault: Journal of Geophysical Research, v. 92, no. B8, p. 7945–7962.

Hudnut, K., and Clark, M., 1989, New slip along parts of the 1968 Coyote Creek Fault rupture, California: Bulletin of the Seismological Society of America, v. 79, p. 451–465.

Kelson, K.I., Lettis, W.R., and Lisowski, M., 1992, Distribution of geologic slip and creep along faults in the San Francisco Bay region, *in* Borchardt, G., Hirschfeld, S.E., Lienkaemper, J.J., McClellan, P., Williams, P.L., and Wong, I.G., eds., Proceedings of the Second Conference on

Earthquake Hazards in the Eastern San Francisco Bay Area: California Department of Conservation, California Division Mines Geology Special Publication 113, p. 31–38.
King, C., Nason, R.D., and Burford, R.O., 1977, Coseismic steps recorded on creep meters along the San Andreas Fault: Journal of Geophysical Research, v. 82, p. 1655–1662.
Lienkaemper, J.J., Baker, B., and McFarland, F.S., 2006, Surface slip associated with the 2004 Parkfield, California, earthquake measured on alinement arrays: Bulletin of the Seismological Society of America, v. 96, no. 4B, p. S239–S249.
Lienkaemper, J.J., Barry, G.R., Smith, F.E., Mello, J.D., and McFarland, F.S., in press 2013, The Greenville Fault—Its long-term creep rate, post-1980-earthquake transient slip, and seismic potential: Bulletin of the Seismological Society of America.
Lienkaemper, J.J., Borchardt, G., and Lisowski, M., 1991, Historical creep rate and potential for seismic slip along the Hayward Fault, California: Journal of Geophysical Research, v. 96, no. B11, p. 18,261–18,283.
Lienkaemper, J.J., Galehouse, J.S., and Simpson, R.W., 2001, Long-term monitoring of creep rate along the Hayward Fault and evidence for a lasting creep response to the 1989 Loma Prieta earthquake: Geophysical Research Letters, v. 28, p. 2265–2268.
Lienkaemper, J.J., and McNutt, M.K,. 2010, Recently active traces of the Bartlett Springs Fault, California—A digital database: U.S. Geological Survey Data Series 541, 13 p.
Lisowski, M., and Prescott, W.H., 1981, Short-range distance measurements along the San Andreas Fault system in central California, 1975 to 1979: Bulletin of the Seismological Society of America, v. 71, no. 5, p. 1607–1624.
Lohman, R.B., and McGuire, J.J., 2007, Earthquake swarms driven by aseismic creep in the Salton Trough, California: Journal of Geophysical Research, v. 112, B04405, doi:10.1029/2006JB004596.
Louie, J.N., Allen, C.R., Johnson, D.C., Haase, P.C., and Cohn, S.N., 1985, Fault slip in southern California: Bulletin of the Seismological Society of America, v. 75, no. 3, p.811–833.
Lyons, S., and Sandwell, D., 2003, Fault creep along the southern San Andreas from interferometric synthetic aperture radar, permanent scatterers, and stacking: Journal of Geophysical Research, v. 108, no. B1, 24 p., doi:10.1029/2002JB001831.
Lyons, S.N., Bock, Y., and Sandwell, D.T., 2002, Creep along the Imperial Fault, southern California, from GPS measurements: Journal of Geophysical Research, v. 107, no. B10, p. ETG12-1–ETG12-13.
Manaker, D.M., Bürgmann, R., and Prescott, W.H., 2003, Distribution of interseismic slip rates and the potential for significant earthquakes on the Calaveras fault, central California: Journal of Geophysical Research, v. 108, no. B6, doi:10.1029/2002JB001749.
McFarland, F.S., Lienkaemper, J.J., and Caskey, S.J., 2007, Data from theodolite measurements of creep rates on San Francisco Bay region faults, California, 1979–2007: U.S. Geological Survey Open-File Report 2007–1367.
McFarland, F.S., Lienkaemper, J.J., and Caskey, S.J., 2009, Data from theodolite measurements of creep rates on San Francisco Bay region faults, California, 1979–2011: U.S. Geological Survey Open-File Report 2009–1119 (v. 1.3, revised 2012).
Murray, J.R., Segall, P., and Cervelli, P., 2001, Inversion of GPS data for spatially variable slip-rate on the San Andreas Fault near Parkfield: Geophysical Research Letters, v. 28, no. 2, p. 359–362.
Murray, J.R., Svarc, J.L., and Minson, S.E., 2012, Spatially variable creep rate on the Bartlett Springs and Maacama Faults, northern California, estimated via Bayesian inversion of Global

Positioning System data [abs.]: Eos (American Geophysical Union Transactions), v. 94, Fall meeting supplement, abs S31A-2488.

Nadeau, R.M., 2007, Periodic pulsing of the San Andreas Fault—An update, *in* Berkeley Seismological Laboratory Annual Reports: Berkeley, University of California, accessed July 26, 2013, at *http://seismo.berkeley.edu/annual_report/ar05_06/node6.html*.

Nadeau, R.M., and McEvilly, T.V., 1999, Fault slip rates at depth from recurrence intervals of repeating microearthquakes: Science, v. 285, p. 718–721.

Nadeau, R.M., and McEvilly, T.V., 2004, Periodic pulsing of characteristic microearthquakes on the San Andreas Fault: Science, v. 303, p. 220–222.

Oppenheimer, D.H., Bakun, W.H., and Lindh, A.G., 1990, Slip partitioning on the Calaveras fault, California, and prospects for future earthquakes: Journal of Geophysical Research, v. 95, p. 8483–8498.

Petersen, M.D., Bryant, W.A., Cramer, C.H., Cao, T., Reichle, M.S., Frankel, A.D., Lienkaemper, J.J., McCrory, P.A., and Schwartz, D.P., 1996, Probabilistic seismic hazard assessment for the state of California: California Geological Survey Open-File Report 96–08, 33 p.

Prescott, W.H., and Burford, R.O., 1976, Slip on the Sargent Fault: Bulletin of the Seismological Society of America, v. 66, no. 3, p. 1013–1016.

Prescott, W.H., Lisowski, M., and Savage, S.C., 1981, Geodetic measurement of crustal deformation on the San Andreas, Hayward, and Calaveras Faults near San Francisco, California: Journal Geophysical Research, v. 86, no. B11, p. 10,853–10,869, doi:10.1029/JB086iB11p10853.

Sandwell, D.T., Sichoix, L., Agnew, D., Bock, Y., and Minster, J.B., 2000, Near real-time radar interferometry of the Mw 7.1 Hector Mine Earthquake: Geophysical Research Letters, v. 27, no. 19, p. 3101–3104.

Savage, J.C., and Lisowski, M., 1993, Inferred depth of creep on the Hayward Fault, central California: Journal of Geophysical Research, v. 98, no. B1, p. 787–793.

Schmidt, D.A., Bürgmann, R., Nadeau, R.M., and d'Alessio, M., 2005, Distribution of aseismic slip rate on the Hayward Fault inferred from seismic and geodetic data: Journal of Geophysical Research, v. 110, no. B08406, doi:10.1029/2004JB003397.

Schulz, S.S., Mavko, G.M., Burford, R.O., and Stuart, W.D., 1982, Long-term fault creep observations in central California: Journal of Geophysical Research, v. 87, no. B8, p. 6977–6982.

Segall, P., 2002, Testing earthquake recurrence models—Space-time patterns of slip-deficit at Parkfield: U.S. Geological Survey National Earthquake Hazard Reduction Program Final Technical Report # 02HQGR0061.

Shirzaei, M., and Bürgmann, R., 2013, Time-dependent model of creep on the Hayward Fault from joint inversion of 18 years of InSAR and surface creep data: Journal of Geophysical Research, v. 118, no. 4, p. 1733–1746, doi:10.1002/jgrb.50149.

Shirzaei, M., Taira, T., and Bürgmann, R., 2013, Implications of recent asperity failures and aseismic creep for time-dependent earthquake hazard on the Hayward Fault; Earth and Planetary Science Letters, p. 371–372, doi:10.1016/j.epsl.2013.1004.1024.

Sieh, K.E., and Williams, P.L., 1990, Behavior of the southernmost San Andreas Fault during the past 300 years: Journal of Geophysical Research, v. 95, no. B5, p. 6629–6645, doi:10.1029/JB095iB05p06629.

Templeton, D.C., Nadeau, R.M., and Burgmann, R., 2008, Behavior of repeating earthquake sequences in central California and implications for subsurface fault creep: Bulletin of the Seismological Society of America, v. 98, no. 1, p. 52–65.

Templeton, D.C., Nadeau, R.M., and Burgmann, R., 2009, Distribution of postseismic slip on the Calaveras Fault, California, following the 1984 M6.2 Morgan Hill earthquake: Earth and Planetary Science Letters, v. 277, p. 1–8.

Titus, S.J., DeMets, C., and Tikoff, B., 2005, New slip rate estimates for the creeping segment of the San Andreas Fault, California: Geology, v. 33, p. 205–208.

Titus, S.J., DeMets, C., and Tikoff, B., 2006, Thirty-five-year creep rates for the creeping segment of the San Andreas Fault and effects of the 2004 Parkfield earthquake—Constraints from alignment arrays, continuous Global Positioning System, and creepmeters: Bulletin of the Seismological Society of America, v. 96, no. 4B, p. S250–S268.

Toké, N.A., Arrowsmith, J.R., Rymer, M.J., Landgraf, A., Haddad, D.E., Busch, M., Coyan, J., and Hannah, A., 2011, Late Holocene slip rate of the San Andreas Fault and its accommodation by creep and moderate-magnitude earthquakes at Parkfield, California: Geology, v. 39, p. 243–246, doi:10.1130/G31498.

Tong, X., Sandwell, D.T., and Smith-Konter, B., 2013, High-resolution interseismic velocity data along the San Andreas Fault from GPS and InSAR: Journal of Geophysical Research, v. 118, no. 1, p. 369-389, doi:10.1029/2012JB009442.

Turner, R.C., Nadeau, R.M., and Bürgmann, R., 2013, Aseismic slip and fault interaction from repeating earthquakes in the Loma Prieta aftershock zone: Geophysical Research Letters, v. 40, no. 6, p. 1079–1083, doi:10.1002/grl.50212.

Wallace, R.E., and Roth, E.F., 1967, Rates and patterns of progressive deformation, *in* The Parkfield-Cholame California Earthquakes of June–August 1966: U.S. Geological Survey Professional Paper 579, p. 23–40.

Wdowinski, S., Smith-Konter, B., Boch, Y., and Sandwell, D., 2007, Diffuse interseismic deformation across the Pacific-North America plate boundary: Geology, v. 35, no. 4, p. 3113–314.

Wei, M., Sandwell, D., and Fialko, Y., 2009, A silent Mw 4.7 slip event of October 2006 on the Superstition Hills Fault, southern California: Journal of Geophysical Research, v. 114, B07402, doi:10.1029/2008JB006135.

Wei, M., Sandwell, D., Fialko, Y., and Bilham, R., 2011, Slip on faults in the Imperial Valley triggered by the 4 April 2010 Mw 7.2 El Mayor-Cucapah earthquake revealed by InSAR: Geophysical Research Letters, v. 38, L01308, doi:10.1029/2010GL045235.

Wei, M., Sandwell, D., and Smith-Konter, B., 2010, Optimal combination of InSAR and GPS for measuring interseismic crustal deformation: Advances in Space Research, v. 46, p. 236–249.

Wesson, R.L., 1988, Dynamics of fault creep: Journal of Geophysical Research, v. 93, p. 8929–8951.

Werner, C.L., Rosen, P., Hensley, S., Fielding, E., and Buckley, S. (not dated), Detection of aseismic creep along the San Andreas Fault near Parkfield, California with ERS-1 Radar interferometry: Pasadena, California, Jet Propulsion Laboratory, accessed July 26, 2012, on the European Space Agency Web site, at *http://earth.esa.int/workshops/ers97/papers/werner*.

Wilmesher, J.F., and Baker, F.B., 1987, Catalog of alignment array measurements in central and southern California from 1983 through 1986: U.S. Geological Survey Open-File Report 87–280, 157 p.

Wills, C.J., Weldon, R.J., II, and Bryant, W.A., 2007, California fault parameters for the National Seismic Hazard Maps and working group on California earthquake probabilities 2007, appendix A *in* 2007 Working Group on California Earthquake Probabilities, The Uniform California Earthquake Rupture Forecast, version 2 (UCERF 2): U.S. Geological Survey Open-File Report 2007–1437-A, and California Geological Survey Special Report 203-A.

Wisely, B.A., Schmidt, D.A., and Weldon, R.J., II, 2007, Compilation of surface creep on California faults and comparison of WG-07 deformation model to Pacific North American plate motion, appendix P *in* 2007 Working Group on California Earthquake Probabilities, The Uniform California Earthquake Rupture Forecast, version 2 (UCERF 2): U.S. Geological Survey Open-File Report 2007–1437-P, and California Geological Survey Special Report 203-P, 63 p.

Table D1. Smoothed creep rate averaged over UCERF minisections.

[Data are sorted by section name. Zero values are for minisections where there are observations that are sufficient to infer that creep is an insignificant fraction of slip rate. All other minisections are assumed to creep at 10 percent of their slip rate (the average ratio for the 249 minisections for which we have data). mm/yr, millimeters per year]

Fault section	Minisection	Smoothed average creep rate (mm/yr)
Bartlett Springs	668.01	0.5
Bartlett Springs	668.02	0.2
Bartlett Springs	668.03	0.0
Bartlett Springs	668.04	0.2
Bartlett Springs	668.05	0.9
Bartlett Springs	668.06	3.0
Bartlett Springs	668.07	6.0
Bartlett Springs	668.08	5.0
Bartlett Springs	668.09	3.0
Bartlett Springs	668.10	1.5
Bartlett Springs	668.11	0.5
Bartlett Springs	668.12	0.3
Bartlett Springs	668.13	0.2
Bartlett Springs	668.14	0.2
Bartlett Springs	668.15	0.1
Bartlett Springs	668.16	0.1
Bartlett Springs	668.17	0.0
Brawley	170.01	([1])
Calaveras (Central)	602.01	13.0
Calaveras (Central)	602.02	9.0
Calaveras (Central)	602.03	8.0
Calaveras (Central)	602.04	7.0
Calaveras (Central)	602.05	5.0
Calaveras (Central)	602.06	3.0
Calaveras (North)	601.01	3.0
Calaveras (North)	601.02	6.0
Calaveras (North)	601.03	4.0
Calaveras (North)	601.04	3.0
Calaveras (North)	601.05	2.0
Calaveras (South) - Paicines extension	621.01	[2]5.0
Calaveras (South) - Paicines extension	621.02	[2]0.5
Calaveras (South) - Paicines extension	621.03	[2]3.0
Calaveras (South) - Paicines extension	621.04	[2]8.0
Calaveras (South) - Paicines extension	621.05	[2]10.0
Calaveras (South) - Paicines extension	621.06	[2]2.0
Calaveras (South)	603.01	8.0
Calaveras (South)	603.02	8.0

Fault section	Minisection	Smoothed average creep rate (mm/yr)
Calaveras (South)	603.03	13.0
Cerro Prieto	172.01	[3]5.0
Cerro Prieto	172.02	[3]5.0
Cerro Prieto	172.03	[3]5.0
Cerro Prieto	172.04	[3]5.0
Cerro Prieto	172.05	[3]5.0
Cerro Prieto	172.06	[3]5.0
Cerro Prieto	172.07	[3]5.0
Cerro Prieto	172.08	[3]5.0
Concord	622.01	3.4
Concord	622.02	3.0
Concord	622.03	1.2
Elsinore - Coyote Mountain	103.01	1.0
Elsinore - Coyote Mountain	103.02	1.0
Elsinore - Coyote Mountain	103.03	1.0
Elsinore - Coyote Mountain	103.04	1.0
Elsinore - Coyote Mountain	103.05	1.0
Garlock (Central)	341.01	0.1
Garlock (Central)	341.02	0.4
Garlock (Central)	341.03	0.5
Garlock (Central)	341.04	0.2
Garlock (Central)	341.05	0.0
Garlock (East)	48.01	0.0
Garlock (East)	48.02	0.0
Garlock (East)	48.03	0.0
Garlock (East)	48.04	0.0
Garlock (West)	49.01	0.1
Garlock (West)	49.02	0.1
Garlock (West)	49.03	0.4
Garlock (West)	49.04	1.8
Garlock (West)	49.05	1.8
Garlock (West)	49.06	1.0
Garlock (West)	49.07	0.9
Garlock (West)	49.08	0.7
Garlock (West)	49.09	0.4
Garlock (West)	49.10	0.2
Green Valley	623.01	3.6
Green Valley	623.02	4.4
Green Valley	623.03	4.4
Green Valley	623.04	3.8

Fault section	Minisection	Smoothed average creep rate (mm/yr)
Greenville (North)	636.01	2.1
Greenville (North)	636.02	2.1
Greenville (North)	636.03	2.1
Greenville (North)	636.04	2.1
Greenville (North)	636.05	2.1
Hayward (North)	639.01	3.9
Hayward (North)	639.02	4.3
Hayward (North)	639.03	4.2
Hayward (North)	639.04	2.5
Hayward (North)	639.05	1.4
Hayward (South)	638.01	1.6
Hayward (South)	638.02	4.6
Hayward (South)	638.03	5.2
Hayward (South)	638.04	4.7
Hayward (South)	638.05	4.0
Hunting Creek - Bartlett Springs connector	677.01	2.0
Hunting Creek - Bartlett Springs connector	677.02	2.0
Hunting Creek - Bartlett Springs connector	677.03	1.8
Hunting Creek - Bartlett Springs connector	677.04	1.3
Hunting Creek - Bartlett Springs connector	677.05	0.8
Hunting Creek - Berryessa	640.01	3.1
Hunting Creek - Berryessa	640.02	2.8
Hunting Creek - Berryessa	640.03	2.6
Hunting Creek - Berryessa	640.04	2.5
Hunting Creek - Berryessa	640.05	2.3
Imperial	97.01	[3]9.0
Imperial	97.02	[3]9.0
Imperial	97.03	[3]9.0
Laguna Salada	104.01	[3]2.0
Laguna Salada	104.02	[3]2.0
Laguna Salada	104.03	[3]2.0
Laguna Salada	104.04	[3]2.0
Laguna Salada	104.05	[3]2.0
Laguna Salada	104.06	[3]2.0
Laguna Salada	104.07	[3]2.0
Laguna Salada	104.08	[3]2.0
Laguna Salada	104.09	[3]2.0
Maacama	644.01	0.0
Maacama	644.02	0.0
Maacama	644.03	2.0

Fault section	Minisection	Smoothed average creep rate (mm/yr)
Maacama	644.04	5.6
Maacama	644.05	3.5
Maacama	644.06	3.0
Maacama	644.07	2.2
Maacama	644.08	1.4
Maacama	644.09	2.2
Maacama	644.10	1.5
Maacama	644.11	0.0
Quien Sabe	648.01	([1])
Quien Sabe	648.01	([1])
Quien Sabe	648.01	([1])
Quien Sabe	648.01	([1])
Rodgers Creek - Healdsburg	651.01	3.5
Rodgers Creek - Healdsburg	651.02	3.0
Rodgers Creek - Healdsburg	651.03	2.2
Rodgers Creek - Healdsburg	651.04	1.8
Rodgers Creek - Healdsburg	651.05	1.9
Rodgers Creek - Healdsburg	651.06	5.0
Rodgers Creek - Healdsburg	651.07	4.4
Rodgers Creek - Healdsburg	651.08	1.6
San Andreas - Carrizo	300.01	0.0
San Andreas - Carrizo	300.02	0.0
San Andreas - Carrizo	300.03	0.0
San Andreas - Carrizo	300.04	0.0
San Andreas - Mojave North	286.01	0.0
San Andreas - Mojave North	286.02	0.0
San Andreas - Mojave North	286.03	0.0
San Andreas - Mojave South	301.01	0.0
San Andreas - Mojave South	301.02	0.0
San Andreas - Mojave South	301.03	0.0
San Andreas - North Coast	654.01	0.0
San Andreas - North Coast	654.02	0.0
San Andreas - North Coast	654.03	0.0
San Andreas - North Coast	654.07	0.0
San Andreas - North Coast	654.10	0.0
San Andreas - North Coast	654.11	0.0
San Andreas - North Coast	654.12	0.0
San Andreas - North Coast	654.13	0.0
San Andreas - North Coast	654.14	0.0
San Andreas - North Coast	654.15	0.0

Fault section	Minisection	Smoothed average creep rate (mm/yr)
San Andreas - North Coast	654.16	0.0
San Andreas - North Coast	654.17	0.0
San Andreas - North Coast	654.18	0.0
San Andreas - North Coast	654.19	0.0
San Andreas - Peninsula	655.01	0.0
San Andreas - Peninsula	655.02	0.0
San Andreas - Peninsula	655.03	0.0
San Andreas - Peninsula	655.04	0.0
San Andreas - Peninsula	655.05	0.0
San Andreas - Peninsula	655.06	0.0
San Andreas - Peninsula	655.07	0.0
San Andreas - Peninsula	655.08	0.0
San Andreas - San Bernardino North	282.01	0.0
San Andreas - San Bernardino North	282.02	0.0
San Andreas - San Bernardino North	282.03	0.0
San Andreas - San Bernardino North	282.04	0.0
San Andreas (Banning)	284.08	0.9
San Andreas (Banning)	284.07	0.9
San Andreas (Banning)	284.06	0.9
San Andreas (Banning)	284.05	0.8
San Andreas (Banning)	284.04	0.8
San Andreas (Banning)	284.03	0.7
San Andreas (Big Bend)	287.01	0.0
San Andreas (Big Bend)	287.02	0.0
San Andreas (Big Bend)	287.03	0.5
San Andreas (Big Bend)	287.04	0.0
San Andreas (Cholame)	285.01	0.0
San Andreas (Cholame)	285.02	0.0
San Andreas (Cholame)	285.03	2.0
San Andreas (Coachella)	295.01	2.5
San Andreas (Creeping Section)	658.01	25.0
San Andreas (Creeping Section)	658.02	25.0
San Andreas (Creeping Section)	658.03	25.0
San Andreas (Creeping Section)	658.04	22.0
San Andreas (Creeping Section)	658.05	24.0
San Andreas (Creeping Section)	658.06	24.0
San Andreas (Creeping Section)	658.07	21.0
San Andreas (Creeping Section)	658.08	21.0
San Andreas (Creeping Section)	658.09	16.0
San Andreas (Creeping Section)	658.10	14.0

Fault section	Minisection	Smoothed average creep rate (mm/yr)
San Andreas (Creeping Section)	658.11	13.0
San Andreas (Parkfield)	32.01	15.0
San Andreas (San Bernardino South)	283.01	0.2
San Andreas (San Bernardino South)	283.02	0.5
San Andreas (San Bernardino South)	283.03	0.6
San Andreas (San Bernardino South)	283.04	0.7
San Andreas (San Bernardino South)	283.05	0.8
San Andreas (San Bernardino South)	283.06	0.9
San Andreas (Santa Cruz Mountains)	657.01	0.0
San Andreas (Santa Cruz Mountains)	657.02	0.0
San Andreas (Santa Cruz Mountains)	657.03	0.0
San Andreas (Santa Cruz Mountains)	657.04	0.0
San Andreas (Santa Cruz Mountains)	657.05	0.0
San Andreas (Santa Cruz Mountains)	657.06	2.0
San Andreas (Santa Cruz Mountains)	657.07	2.0
San Andreas (Santa Cruz Mountains)	657.08	8.0
San Andreas (Santa Cruz Mountains)	657.09	8.0
San Gregorio (North)	660.07	0.0
San Gregorio (North)	660.09	0.5
San Gregorio (North)	660.10	1.0
San Gregorio (North)	660.11	0.5
San Jacinto (Anza)	293.01	1.6
San Jacinto (Anza)	293.02	0.8
San Jacinto (Anza)	293.03	0.2
San Jacinto (Borrego)	99.01	1.4
San Jacinto (Borrego)	99.02	2.0
San Jacinto (Borrego)	99.03	4.0
San Jacinto (Borrego)	99.04	5.5
San Jacinto (Borrego)	99.05	5.5
San Jacinto (Coyote Creek)	101.01	0.0
San Jacinto (Coyote Creek)	101.02	0.0
San Jacinto (Coyote Creek)	101.03	0.6
San Jacinto (San Bernardino)	119.01	1.0
San Jacinto (San Bernardino)	119.02	2.5
San Jacinto (San Bernardino)	119.03	1.0
San Jacinto (San Jacinto Valley)	289.01	0.1
San Jacinto (San Jacinto Valley)	289.02	0.1
San Jacinto (Stepovers Combined)	401.01	1.2
San Jacinto (Superstition Hills)	98.01	3.3
San Jacinto (Superstition Hills)	98.02	2.0

Fault section	Minisection	Smoothed average creep rate (mm/yr)
San Jacinto (Superstition Hills)	98.03	1.0
Sargent	662.01	0.4
Sargent	662.02	1.1
Sargent	662.03	1.9
Sargent	662.04	2.7
Sargent	662.05	2.9
Sargent	662.06	2.9
West Napa	665.01	0.0
West Napa	665.02	0.1
West Napa	665.03	0.0
West Napa	665.04	0.0

[1]Special case; use 90 percent of slip rate for all deformation models.

[2]Paicines rates were smoothed and tapered to match strain transfer between fault zones.

[3]Recorded single value; creep rate is tapered proportionally to the slip rate in model.

Table D2. Raw observations.

[Creep rate and uncertainty ("sig" or 1-sigma) are given in millimeters per year (mm/yr); Inst, instrument used for measurement; AA, alignment array; Geod, geodelite; CM, creep meter; SAR, synthetic aperture radar; Cult, cultural feature, Tran, transit; Trilat, trilateral array]

Longitude	Latitude	Location	Creep rate (mm/yr)	sig (mm/yr)	Type	Inst	Start	End	Years	Source	Comments
Calaveras											
-121.9598	37.7458	Upper North	0.2	0.1	Int	AA	1980	1989	9	Galehouse and Lienkaemper (2003)	Pre-Loma Prieta rate
-121.9359	37.7044	Camp Parks	2.8	0.5	Int	AA	1965	1977	12	Lisowski and Prescott (1981)	
-121.8642	37.581	Veras	2.9	0.3	Int	Geod	1965	1976	11	Prescott and others (1981)	
-121.8508	37.5358	Lower North	3.6	0.5	Int	AA	1997	2001	4	Galehouse and Lienkaemper (2003)	Post-LP
-121.812	37.4578	Reservoir	2.2	0.5	Int	Geod	1970	1979	9	Prescott and others (1981)	
-121.7139	37.3417	Grant Ranch	9.4	0.4	Int+Aft	Geod	1977	1984	7	Oppenheimer and others (1990)	Post-Coyote Lake
-121.5242	37.0699	Central	14	2	Int	AA	1968	1989	21	Galehouse and Lienkaemper (2003)	Corrected for MH/CL events
-121.4826	37.0096	San Felipe	13	2	Int	Geod	1972	1979	7	Lisowski and Prescott (1981)	
-121.4128	36.8699	Wright Rd	13	Undefined	Int+Aft	CM	1971	1983	12	Schulz and others (1982)	Post-Coyote Lake
-121.4128	36.8496	C-SA Junct	12.2	0.2	Int+Aft	AA	1979	1989	10	Galehouse and Lienkaemper (2003)	Pre-LP; post MH/CL
-121.4053	36.8496	C-SA Junct	6.4	0.2	Int+Aft	AA	1979	1989	10	Galehouse and Lienkaemper (2003)	Pre-LP; post MH/CL
-121.3736	36.805	Paicines-Tres P.	5	3	Int	Geod	1975	1979	4	Lisowski and Prescott (1981)	
-121.3233	36.805	Paicines-Thomas	6.2	0.1	Int	AA	1973	1986	13	Wilmesher and Baker (1987)	
-121.1425	36.5932	Paicines-Pionne	10	3	Int	Geod	1975	1979	4	Lisowski and Prescott (1981)	
-121.40631	36.84952	Seventh Street	6.8	0.05					30.6	McFarland and others (2011)	
-121.96083	37.74569	Corey Place	1.8	0.05					29.4	McFarland and others (2011)	
-121.52521	37.06981	Coyote Ranch	17.1	0.21					42.1	McFarland and others (2011)	
-121.71616	37.34233	Halls Valley	1.1	Unknown					1.2	McFarland and others (2011)	
-121.80389	37.44606	Marsh Road	-7.1	Unknown					1.2	McFarland and others (2011)	
-121.93713	37.70649	Shannon Park	1.8	0.45					8.5	McFarland and others (2011)	
-121.87693	37.5985	Sunol	1.8	0.36					7.8	McFarland and others (2011)	
-121.85183	37.5357	Welch Creek Road	4.4	0.1					13.5	McFarland and others (2011)	
-121.41381	36.86982	Wright Road	9	0.08					30.6	McFarland and others (2011)	
-121.189	36.628		7.42	2.063		SAR	2006	2010		Tong and others (2013)	
-121.266	36.697		-0.533	1.552		SAR	2006	2010		Tong and others (2013)	
-121.339	36.766		0.427	1.598		SAR	2006	2010		Tong and others (2013)	
-121.396	36.842		5.19	2.051		SAR	2006	2010		Tong and others (2013)	
-121.436	36.924		8.88	11.067		SAR	2006	2010		Tong and others (2013)	
-121.483	37.005		7.157	2.284		SAR	2006	2010		Tong and others (2013)	
-121.538	37.084		25.304	2.426		SAR	2006	2010		Tong and others (2013)	
-121.598	37.161		9.22	1.458		SAR	2006	2010		Tong and others (2013)	
-121.656	37.238		-3.419	1.843		SAR	2006	2010		Tong and others (2013)	
-121.712	37.315		-3.855	4.634		SAR	2006	2010		Tong and others (2013)	
-121.768	37.392		4.576	1.833		SAR	2006	2010		Tong and others (2013)	
-121.819	37.473		-4.378	5.807		SAR	2006	2010		Tong and others (2013)	

Longitude	Latitude	Location	Creep rate (mm/yr)	sig (mm/yr)	Type	Inst	Start	End	Years	Source	Comments
-121.859	37.557		14.671	6.272		SAR	2006	2010		Tong and others (2013)	
-121.902	37.64		-2.585	2.477		SAR	2006	2010		Tong and others (2013)	
-121.945	37.721		4.922	1.95		SAR	2006	2010		Tong and others (2013)	
		Morgan Hill	15.2							Templeton and others (2009)	Average slip rate

Garlock

Longitude	Latitude	Location	Creep rate (mm/yr)	sig (mm/yr)	Type	Inst	Start	End	Years	Source	Comments
-118.299	35.0898	Cameron	5.7	1.5	Int	AA	1971	1982		Louie and others (1985)	spread over 200 m zone
-117.656	35.452	Rand	0	Undefined	Int	AA	1971	1983		Louie and others (1985)	<0.1; locked east of Keohn Lake
-117.352	35.532	Christmas	0	Undefined	Int	AA	1971	1983		Louie and others (1985)	<0.5 mm/yr
-118.867	34.826		0.448	0.532		SAR	2006	2010		Tong and others (2013)	
-118.771	34.881		0.954	0.543		SAR	2006	2010		Tong and others (2013)	
-118.676	34.924		0.366	0.572		SAR	2006	2010		Tong and others (2013)	
-118.578	34.965		-0.619	0.305		SAR	2006	2010		Tong and others (2013)	
-118.479	34.995		1.717	0.609		SAR	2006	2010		Tong and others (2013)	
-118.386	35.044		-0.349	0.477		SAR	2006	2010		Tong and others (2013)	
-118.296	35.098		-1.688	0.419		SAR	2006	2010		Tong and others (2013)	
-118.203	35.145		0.518	0.261		SAR	2006	2010		Tong and others (2013)	
-118.112	35.19		-0.025	0.077		SAR	2006	2010		Tong and others (2013)	
-118.025	35.246		0.073	0.593		SAR	2006	2010		Tong and others (2013)	
-117.944	35.309		-2.065	2.262		SAR	2006	2010		Tong and others (2013)	
-117.86	35.368		0.255	1.099		SAR	2006	2010		Tong and others (2013)	
-117.766	35.412		0.042	0.255		SAR	2006	2010		Tong and others (2013)	
-117.665	35.449		0.548	0.15		SAR	2006	2010		Tong and others (2013)	
-117.561	35.477		0.467	0.252		SAR	2006	2010		Tong and others (2013)	
-117.456	35.504		-0.32	0.055		SAR	2006	2010		Tong and others (2013)	
-117.349	35.526		0.302	0.187		SAR	2006	2010		Tong and others (2013)	
-117.242	35.551		1.583	0.219		SAR	2006	2010		Tong and others (2013)	
-117.136	35.575		0.516	0.19		SAR	2006	2010		Tong and others (2013)	
-117.029	35.595		-0.702	0.21		SAR	2006	2010		Tong and others (2013)	
-116.92	35.604		-0.36	0.097		SAR	2006	2010		Tong and others (2013)	
-116.81	35.596		-0.088	0.091		SAR	2006	2010		Tong and others (2013)	
-116.7	35.593		-0.869	0.483		SAR	2006	2010		Tong and others (2013)	
-116.59	35.591		0.068	0.092		SAR	2006	2010		Tong and others (2013)	

Concord

Longitude	Latitude	Location	Creep rate (mm/yr)	sig (mm/yr)	Type	Inst	Start	End	Years	Source	Comments
-122.037	37.9758	Concord – Salvio Street	2.9	0.03	Int	AA	1979	2009	30	McFarland and others (2011)	
-122.034	37.972	Concord - Ashbury Drive	3.7	0.03	Int	AA	1979	2009	30	McFarland and others (2011)	
-122.036	37.972		1.738	5.099		SAR	2006	2010	4	Tong and others (2013)	

Longitude	Latitude	Location	Creep rate (mm/yr)	sig (mm/yr)	Type	Inst	Start	End	Years	Source	Comments
Hayward											
-122.3546	37.9891		5	0.1	Int	AA	1968.333	1993.058	24.725	Lienkaemper and others (2001)	
-122.3379	37.969		4.8	0.2	Int	AA	1980.609	1999.89	19.281	Lienkaemper and others (2001)	
-122.3083	37.9425		4.9	0.4	Int	AA	1989.748	1999.677	9.929	Lienkaemper and others (2001)	
-122.2918	37.9246		4.4	0.3	Int	AA	1989.748	1999.868	10.12	Lienkaemper and others (2001)	
-122.2506	37.8719		4.6	0.1	Int	AA	1966.912	1999.658	32.746	Lienkaemper and others (2001)	
-122.2304	37.8484		3.8	0.1	Int	AA	1974.258	1999.696	25.438	Lienkaemper and others (2001)	
-122.209	37.8264		3.7	0.2	Int	AA	1993.112	1999.89	6.778	Lienkaemper and others (2001)	
-122.1975	37.8101		3.7	0.1	Int	AA	1970.29	1999.696	29.406	Lienkaemper and others (2001)	
-122.1882	37.7951		3.6	0.3	Int	AA	1974.274	1999.66	25.386	Lienkaemper and others (2001)	
-122.1504	37.7546		3.7	0.5	Int	AA	1989.693	1999.888	10.195	Lienkaemper and others (2001)	
-122.1285	37.7319		5.9	0.5	Int	AA	1993.389	1999.679	6.29	Lienkaemper and others (2001)	
-122.1045	37.695		5.5	0.9	Int	AA	1992.62	1999.66	7.04	Lienkaemper and others (2001)	
-122.0899	37.6798		5	0.1	Int	AA	1967.167	1999.83	32.663	Lienkaemper and others (2001)	
-122.0804	37.6703		4.4	0.1	Int	AA	1980.478	1999.83	19.352	Lienkaemper and others (2001)	
-122.0727	37.6627		4	0.6	Int	AA	1977.074	1999.677	22.603	Lienkaemper and others (2001)	
-122.0579	37.6481		6.7	0.5	Int	AA	1994.589	1999.677	5.088	Lienkaemper and others (2001)	
-122.0222	37.6143		5.1	0.7	Int	AA	1994.592	1999.696	5.104	Lienkaemper and others (2001)	
-122.0008	37.5925		5.1	0.2	Int	AA	1979.729	1999.83	20.101	Lienkaemper and others (2001)	
-121.9797	37.5664		6	1.3	Int	AA	1983.759	1988.847	5.088	Lienkaemper and others (2001)	
-121.9607	37.5422		5.6	0.3	Int	AA	1979.726	1989.808	10.082	Lienkaemper and others (2001)	
-121.9548	37.5361		8.9	0.6	Int	Cult	1940.3	1987.636	47.336	Lienkaemper and others (2001)	Creep stopped following Loma Prieta
-121.9343	37.5125		9.5	0.6	Int	Cult	1967.7	1987.636	19.936	Lienkaemper and others (2001)	Creep stopped following Loma Prieta
-121.9316	37.5097		8.2	0.4	Int	Cult	1968.7	1982.3	13.6	Lienkaemper and others (2001)	Creep stopped following Loma Prieta
-121.949	37.526		5.708	1.137		SAR	2006	2010	4	Tong and others (2013)	
-122.012	37.601		2.505	0.946		SAR	2006	2010	4	Tong and others (2013)	
-122.083	37.673		2.907	0.528		SAR	2006	2010	4	Tong and others (2013))	
-122.143	37.746		1.291	0.586		SAR	2006	2010	4	Tong and others (2013))	
-122.21	37.821		3.554	0.297		SAR	2006	2010	4	Tong and others (2013))	
-122.27	37.896		4.91	0.718		SAR	2006	2010	4	Tong and others (2013))	
-122.33902	37.96918	Contra Costa College	5.2	0.01					30.2	McFarland and others (2011)	
-122.30959	37.94252	Olive Drive	5.3	0.08					21.1	McFarland and others (2011)	
-122.29294	37.92449	Thors Bay Road	3.4	0.09					21.1	McFarland and others (2011)	
-122.2734	37.8998	Florida Avenue	2.7	0.06					13.2	McFarland and others (2011)	
-122.25061	37.87066	Memorial Stadium	4.7	0.03					44	McFarland and others (2011)	
-122.24107	37.86447	Dwight Way	5	0.26					13.2	McFarland and others (2011)	
-122.23137	37.84853	Temescal	4.1	0.11					36.5	McFarland and others (2011)	

Longitude	Latitude	Location	Creep rate (mm/yr)	sig (mm/yr)	Type	Inst	Start	End	Years	Source	Comments
-122.21005	37.82638	LaSalle Ave	4	0.06					17.7	McFarland and others (2011)	
-122.19863	37.80999	Lincoln	3.6	0.1					40.5	McFarland and others (2011)	
-122.18931	37.79504	39th	4.2	0.14					36.5	McFarland and others (2011)	
-122.16977	37.77426	73rd	3.4	0.11					16.4	McFarland and others (2011)	
-122.15148	37.75453	Encina Way	2.5	0.09					21.1	McFarland and others (2011)	
-122.12993	37.73184	Chabot Park	4	0.15					17.4	McFarland and others (2011)	
-122.12131	37.71749	Fairmont	3.9	0.22					13.2	McFarland and others (2011)	
-122.10578	37.69495	167th	4.7	0.09					18.2	McFarland and others (2011)	
-122.09121	37.67983	Rose Street	4.6	0.04					30.3	McFarland and others (2011)	
-122.08162	37.67021	D Street	4.5	0.02					30.3	McFarland and others (2011)	
-122.07397	37.6627	Palisade	4.7	0.19					33.7	McFarland and others (2011)	
-122.05902	37.64798	Sepulchre	5.5	0.09					16.2	McFarland and others (2011)	
-122.0414	37.63097	Woodland	4.4	0.11					40.7	McFarland and others (2011)	
-122.02325	37.61422	Chimes	6.4	0.17					16.2	McFarland and others (2011)	
-122.00193	37.5924	Appian Way	5.7	0.04					31.1	McFarland and others (2011)	
-121.98094	37.56645	Gilbert	5.4	0.13					27.1	McFarland and others (2011)	
-121.96187	37.5421	Rockett Drive	5.4	0.06					31	McFarland and others (2011)	
-121.95914	37.53942	Hancock	6	0.18					28.7	McFarland and others (2011)	
-121.95584	37.53614	Union	6.6	0.11					17.8	McFarland and others (2011)	
-121.94181	37.51973	Pine	6.3	0.2					21.6	McFarland and others (2011)	
-121.93528	37.51235	Camellia Drive	4.5	0.1					20.7	McFarland and others (2011)	
-121.93262	37.5096	Parkmeadow Drive	6.1	0.09					18.5	McFarland and others (2011)	
-121.93046	37.5072	S. Grimmer	5.9	0.23					28.3	McFarland and others (2011)	
-121.92894	37.50516	Onondaga	2.9	0.22					28.4	McFarland and others (2011)	
-121.92182	37.49629	Mission	5	0.17					16.6	McFarland and others (2011)	
Imperial											
-115.356	32.683	Tuttle Ranch	1	Undefined	Int	?	?	1977		Goulty and others (1978)	Pre-EQ rate
-115.356	32.683	Tuttle Ranch	1.4	Undefined	Int	CM	1975	1979		Louie and others (1985)	Pre-EQ rate
-115.356	32.683	Tuttle Ranch	6	Undefined	Aft	CM	1980	1984		Louie and others (1985)	Afterslip from 1979 event
-115.4787	32.8202	Ross Road	5	Undefined	Int	CM	?	1979		Louie and others (1985)	
-115.51	32.862	Worthington Road	13	8	Int	AA	1974	1979		Louie and others (1985)	
-115.488	32.837	S80	5.4	Undefined	Int+Tran	AA	1967	1978		Louie and others (1985)	Triggered by 1968 EQ

Longitude	Latitude	Location	Creep rate (mm/yr)	sig (mm/yr)	Type	Inst	Start	End	Years	Source	Comments
Maacama											
-123.3559	39.4125	W. Comm	5.8	0.08	Int	AA	1991	2009	18	McFarland and others (2011)	
-123.1664	39.1392	Sanford R.	4.3	0.08	Int	AA	1993	2009	16	McFarland and others (2011)	
-123.0507	38.93464	Middle Ridge	6.1	3.7					2.2	McFarland and others (2011)	
-122.82647	38.7032	Skipstone Ranch	-0.1	1.5					2.4	McFarland and others (2011)	
-122.922	38.786		4.794	1.988		SAR	2006	2010	4	Tong and others (2013)	
-122.993	38.859		-1.683	1.067		SAR	2006	2010	4	Tong and others (2013)	
-123.048	38.937		8.481	5.452		SAR	2006	2010	4	Tong and others (2013)	
-123.095	39.018		2.445	1.547		SAR	2006	2010	4	Tong and others (2013)	
-123.143	39.1		2.749	1.301		SAR	2006	2010	4	Tong and others (2013)	
-123.191	39.181		3.014	1.027		SAR	2006	2010	4	Tong and others (2013)	
-123.248	39.26		-7.65	2.828		SAR	2006	2010	4	Tong and others (2013)	
-123.305	39.339		0.846	2.7		SAR	2006	2010	4	Tong and others (2013)	
-123.353	39.42		-6.367	6.17		SAR	2006	2010	4	Tong and others (2013)	
-123.401	39.502		-8.432	6.456		SAR	2006	2010	4	Tong and others (2013)	
-123.451	39.584		-13.417	3.456		SAR	2006	2010	4	Tong and others (2013)	
-123.502	39.665		0.2	1.696		SAR	2006	2010	4	Tong and others (2013)	
-123.557	39.744		-0.966	1.532		SAR	2006	2010	4	Tong and others (2013)	
		Hopland	6.1	3.7						See Lienkaemper email	
		Alexander Vy	-0.1	1.5						See Lienkaemper email	
		Willits	5.8	0.1						See Lienkaemper email	
		Ukiah	4.3	0.1						See Lienkaemper email	
Rodgers Creek											
-122.7083	38.4701	Nielson Rd	0.4	0.5	Int	AA	1980	1986	6	Galehouse and Lienkaemper (2003)	
-122.6405	38.3478	Roberts Rd	1.6	0.1	Int	AA	1986	2000	14	Galehouse and Lienkaemper (2003)	site not on active trace
-122.4469	38.0987	San Pablo	1.4	1.1	Int	Trilat	1978	1988	10	Lienkaemper and others (1991)	
-122.449	38.17		3.851	3.335		SAR	2006	2010	4	Tong and others (2013)	
-122.52	38.242		-2.919	1.955		SAR	2006	2010	4	Tong and others (2013)	
-122.594	38.313		-3.24	1.706		SAR	2006	2010	4	Tong and others (2013)	
-122.654	38.387		2.083	2.017		SAR	2006	2010	4	Tong and others (2013)	
-122.712	38.465		3.222	1.252		SAR	2006	2010	4	Tong and others (2013)	
-122.7175	38.47995	Fountaingrove Blvd	-0.7	1.1					1.5	McFarland,Lienkaemper,Caskey (2011)	
-122.73807	38.50169	Mark West Springs Rd	6.1	4.2					2.4	McFarland,Lienkaemper,Caskey (2011)	
-122.69446	38.43687	Solano Drive	1.7	0.13					7.7	McFarland,Lienkaemper,Caskey (2011)	
-122.59046	38.30928	Sonoma Mtn Rd	1.3	0.39					7.7	McFarland,Lienkaemper,Caskey (2011)	

Longitude	Latitude	Location	Creep rate (mm/yr)	sig (mm/yr)	Type	Inst	Start	End	Years	Source	Comments
San Andreas											
-123.6895	39	Point Arena	0.5	0.1	Int	AA	1981	2000	19	Galehouse and Lienkaemper (2003)	includes LP, coords approx
-122.7969	38.0441	Point Reyes	-0.1	0	Int	AA	1985	2009	24	McFarland and others (2011)	includes LP
-122.4646	37.6443	SF Penn	-0.3	0.02	Int	AA	1980	1994	14	Galehouse and Lienkaemper (2003)	includes LP
-122.2605	37.4171	SF Penn	0.3	0.1	Int	AA	1989	2000	11	Galehouse and Lienkaemper (2003)	includes LP
-121.5851	36.8827	SJB	0.1	0.1	Int	AA	1989	1998	9	Galehouse and Lienkaemper (2003)	includes LP
-121.5207	36.8351	SJB	10.4	0.2	Int	AA	1990	2001	11	Galehouse and Lienkaemper (2003)	accelerated by Loma Prieta?
-121.6483	36.9267	Chamberland	0.8	0.4	Int	AA	1967	1972	5	Burford and Harsh (1980)	End point
-121.52	36.8367	San Juan	14	0.4	Int	AA	1968	1977	9	Burford and Harsh (1980)	End point
-121.3467	36.72	Paicines	13.5	0.4	Int	AA	1972	1977	5	Burford and Harsh (1980)	End point
-121.2717	36.6583	Lewis	14	0.4	Int	AA	1973	1977	4	Burford and Harsh (1980)	End point
-121.2017	36.605	Cross-Willow	19.9	0.4	Int	AA	1972	1977	5	Burford and Harsh (1980)	End point
-121.185	36.595	Willow Creek	22.7	0.4	Int	AA	1972	1977	5	Burford and Harsh (1980)	End point
-121.1845	36.5933	Melendy	22.9	0.4	Int	AA	1967	1978	11	Burford and Harsh (1980)	End point
-121.1835	36.574	River Terrace	23.1	0.4	Int	AA	1970	1973	3	Burford and Harsh (1980)	Block faulting
-121.135	36.5433	Pinnacles	23.1	0.4	Int	AA	1972	1977	5	Burford and Harsh (1980)	End point
-121.0517	36.4817	Dry Lake	21.9	0.4	Int	AA	1967	1974	7	Burford and Harsh (1980)	End point
-120.975	36.3883	Eade Ranch	31.3	0.4	Int	AA	1970	1976	6	Burford and Harsh (1980)	End point
-120.9693	36.3833	Smith Ranch	33.3	0.4	Int	AA	1967	1971	4	Burford and Harsh (1980)	End point
-120.9017	36.3167	DeAlvarez	31.4	0.4	Int	AA	1970	1977	7	Burford and Harsh (1980)	End point
-120.7983	36.2133	Monarch Peak	17.3	0.4	Int	AA	1968	1977	9	Burford and Harsh (1980)	End point
-120.7567	36.18	Mee Ranch	26	0.4	Int	AA	1970	1977	7	Burford and Harsh (1980)	End point
-120.6283	36.065	Slack Canyon	30	0.4	Int	AA	1968	1979	11	Burford and Harsh (1980)	End point
-120.5717	36.015	Bagby ranch	23.8	0.4	Int	AA	1970	1979	9	Burford and Harsh (1980)	End point
-120.4217	35.885	Durham Ranch	14.6	0.4	Int	AA	1968	1979	11	Burford and Harsh (1980)	End point
-120.3071	35.7566	Water tank	4	0.4	Int	AA	1966	1979	13	Burford and Harsh (1980)	End point
-120.205	35.6517	Palo Prieto	0	0.4	Int	AA	1975	1977	2	Burford and Harsh (1980)	<1 mm/yr
-121.5453	36.8549	Nyland Fence	8	0.2	Int	Cult	1942	1978	36	Burford and Harsh (1980)	
-121.525	36.8392	Old Highway	13.3	0.2	Int	Cult	1926	1978	52	Burford and Harsh (1980)	
-121.3839	36.7495	Cienega Winery	12.3	0.2	Int	Cult	1948	1976	28	Burford and Harsh (1980)	
-121.1943	36.5988	Fence, Airline	19	0.2	Int	Cult	1937	1966	29	Brown and Wallace (1968)	
-121.1841	36.5902	Corral, Melendy	22	0.2	Int	Cult	1945	1978	33	Burford and Harsh (1980)	
-121.163	36.5735	Wire, Melendy	8	0.2	Int	Cult	1951	1966	15	Brown and Wallace (1968)	
-120.9823	36.3972	Lane, BWV	25	0.2	Int	Cult	1908	1966	58	Brown and Wallace (1968)	
-120.9687	36.3828	Fence, BWV	28	0.2	Int	Cult	1941	1966	25	Brown and Wallace (1968)	
-120.5357	35.9837	Fence, Claassen	25	0.2	Int	Cult	1946	1966	20	Wallace and Roth (1967)	
-120.4337	35.8951	Parkfield Brdg	22	0.2	Int	Cult	1932	1978	46	Burford and Harsh (1980)	
-120.3072	35.7567	Fence, Cholame	18	0.2	Int	Cult	1908	1978	70	Burford and Harsh (1980)	
-120.2267	35.6728	Fence, O'Brien L	0	0.2	Int	Cult	1937	1966	29	Brown and Wallace (1968)	

Longitude	Latitude	Location	Creep rate (mm/yr)	sig (mm/yr)	Type	Inst	Start	End	Years	Source	Comments
-120.969	36.3883	Smith Ranch	23.2	1	Int	GPS	1967	2003	36	Titus and others (2005)	End point
-120.798	36.18	Mee Ranch	26.7	1	Int	GPS	1970	2003	33	Titus and others (2005)	End point
-120.628	36.065	Slack Cny	24.9	1	Int	GPS	1968	2003	35	Titus and others (2005)	End point
-121.39	36.75	Cienega Winery	12.3	Undefined	Int	CM	1958	1976	18	Burford (1988)	includes triggered creep
-121.5	36.82	SJN	8.1	Undefined	Int	CM	1969	1976	7	Burford (1988)	includes triggered creep
-121.52	36.84	XSJ1/2	9	Undefined	Int	CM	1969	1976	7	Burford (1988)	includes triggered creep
-121.42	36.77	HRS	10.9	Undefined	Int	CM	1969	1976	7	Burford (1988)	includes triggered creep
-121.23	36.65	SCR	13.8	Undefined	Int	CM	1969	1976	7	Burford (1988)	includes triggered creep
-121.19	36.6	XMR1	20.3	Undefined	Int	CM	1969	1976	7	Burford (1988)	includes triggered creep
-121.18	36.59	MRB	21.2	Undefined	Int	CM	1969	1976	7	Burford (1988)	includes triggered creep
-120.63	36.07	XSC1	22.1	Undefined	Int	CM	1972	1987	15	Burford (1988)	includes triggered creep
-120.42	35.88	XDR2	8.3	Undefined	Int	CM	1972	1987	15	Burford (1988)	includes triggered creep
-120.36	35.84	CRR1	3.97	Undefined	Int	CM	1971	1987	16	Burford (1988)	includes triggered creep
-120.35	35.82	XGH1	3.25	Undefined	Int	CM	1972	1987	15	Burford (1988)	includes triggered creep
-118.11	34.55	Una Lake	0	0.5	Int	AA	1970	1984	14	Louie and others (1985)	below instrument uncertainty
-117.888	34.457	Pallett Creek	0	0.2	Int	AA	1970	1984	14	Louie and others (1985)	below instrument uncertainty
-117.8	34.422	Big Pines	0	1	Int	AA	1970	1981	11	Louie and others (1985)	below instrument uncertainty
-117.49	34.2858	Cajon	0	0.5	Int	AA	1970	1984	14	Louie and others (1985)	< 1cm of creep
-117.276	34.174	Waterman	0	1	Int	AA	1970	1983	13	Louie and others (1985)	below instrument uncertainty
-116.964	34.058	Santa Ana wash	0	0.4	Int	AA	1970	1983	13	Louie and others (1985)	below instrument uncertainty
-116.616	33.9325	Devers	2	Undefined	Int	AA	1972	1982	10	Louie and others (1985)	
-116.234	33.777	Indio	1.5	0.6	Int	AA	1970	1984	14	Louie and others (1985)	
-115.887	33.482	Mecca beach	0.7	Undefined	Int	CM	1981	1984	3	Louie and others (1985)	
-115.949	33.541	North Shore	0	0.1	Int	CM	1970	1984	14	Louie and others (1985)	below instrument uncertainty
-115.99	33.58	Red Canyon	1.7	Undefined	Aft	AA	1967	1983	16	Louie and others (1985)	afterslip from 1968 EQ?
-116.156	33.715	Dillon road	2	1	Int+Tran	AA	1970	1984	14	Louie and others (1985)	triggered by 1979 EQ?
-115.724	33.349		0.025	0.73		SAR	2006	2010	4	Tong and others (2013)	
-115.799	33.416		4.074	0.629		SAR	2006	2010	4	Tong and others (2013)	
-115.877	33.475		0.018	1.242		SAR	2006	2010	4	Tong and others (2013)	
-115.951	33.542		4.299	0.802		SAR	2006	2010	4	Tong and others (2013)	
-116.026	33.608		4.076	0.241		SAR	2006	2010	4	Tong and others (2013)	
-116.102	33.669		4.762	0.642		SAR	2006	2010	4	Tong and others (2013)	
-116.178	33.734		4.005	1.11		SAR	2006	2010	4	Tong and others (2013)	
-116.255	33.796		0.139	0.138		SAR	2006	2010	4	Tong and others (2013)	
-116.336	33.856		0.876	0.298		SAR	2006	2010	4	Tong and others (2013)	
-116.422	33.907		0.939	0.396		SAR	2006	2010	4	Tong and others (2013)	
-116.508	33.962		-0.618	0.41		SAR	2006	2010	4	Tong and others (2013)	
-116.6	34.013		-0.598	0.393		SAR	2006	2010	4	Tong and others (2013)	
-116.701	34.042		0.624	0.691		SAR	2006	2010	4	Tong and others (2013)	

Longitude	Latitude	Location	Creep rate (mm/yr)	sig (mm/yr)	Type	Inst	Start	End	Years	Source	Comments
-116.806	34.063		1.089	1.413		SAR	2006	2010	4	Tong and others (2013)	
-116.912	34.078		2.02	1.637		SAR	2006	2010	4	Tong and others (2013)	
-117.017	34.101		-0.404	1.915		SAR	2006	2010	4	Tong and others (2013)	
-117.121	34.124		0.081	0.537		SAR	2006	2010	4	Tong and others (2013)	
-117.223	34.151		0.013	0.326		SAR	2006	2010	4	Tong and others (2013)	
-117.319	34.194		0.346	0.505		SAR	2006	2010	4	Tong and others (2013)	
-117.411	34.245		0.116	0.59		SAR	2006	2010	4	Tong and others (2013)	
-117.503	34.292		-1.904	1.885		SAR	2006	2010	4	Tong and others (2013)	
-117.597	34.339		-5.121	5.177		SAR	2006	2010	4	Tong and others (2013)	
-117.694	34.378		-1.187	1.673		SAR	2006	2010	4	Tong and others (2013)	
-117.791	34.418		-2.074	0.611		SAR	2006	2010	4	Tong and others (2013)	
-117.888	34.457		-0.901	0.103		SAR	2006	2010	4	Tong and others (2013)	
-117.985	34.498		0.056	0.241		SAR	2006	2010	4	Tong and others (2013)	
-118.082	34.539		-1.64	0.509		SAR	2006	2010	4	Tong and others (2013)	
-118.181	34.578		-0.798	0.304		SAR	2006	2010	4	Tong and others (2013)	
-118.28	34.616		-1.602	0.884		SAR	2006	2010	4	Tong and others (2013)	
-118.379	34.652		-1.176	1.137		SAR	2006	2010	4	Tong and others (2013)	
-118.48	34.688		-5.093	0.956		SAR	2006	2010	4	Tong and others (2013)	
-118.582	34.719		-2.272	1.089		SAR	2006	2010	4	Tong and others (2013)	
-118.685	34.749		-0.701	0.982		SAR	2006	2010	4	Tong and others (2013)	
-118.789	34.777		-1.425	0.675		SAR	2006	2010	4	Tong and others (2013)	
-118.893	34.808		-1.755	0.681		SAR	2006	2010	4	Tong and others (2013)	
-118.998	34.824		-1.012	0.345		SAR	2006	2010	4	Tong and others (2013)	
-119.105	34.846		1.344	0.444		SAR	2006	2010	4	Tong and others (2013)	
-119.211	34.86		0.298	0.413		SAR	2006	2010	4	Tong and others (2013)	
-119.312	34.895		2.101	0.872		SAR	2006	2010	4	Tong and others (2013)	
-119.405	34.941		-0.85	0.765		SAR	2006	2010	4	Tong and others (2013)	
-119.492	34.998		-1.631	0.274		SAR	2006	2010	4	Tong and others (2013)	
-119.575	35.057		-1.647	0.844		SAR	2006	2010	4	Tong and others (2013)	
-119.655	35.12		-0.175	0.565		SAR	2006	2010	4	Tong and others (2013)	
-119.732	35.183		0.602	1.22		SAR	2006	2010	4	Tong and others (2013)	
-119.805	35.25		0.016	2.546		SAR	2006	2010	4	Tong and others (2013)	
-119.877	35.319		0.609	0.857		SAR	2006	2010	4	Tong and others (2013)	
-119.946	35.387		0.8	0.885		SAR	2006	2010	4	Tong and others (2013)	
-120.013	35.461		-0.593	2.139		SAR	2006	2010	4	Tong and others (2013)	
-120.081	35.531		0.338	0.987		SAR	2006	2010	4	Tong and others (2013)	
-120.152	35.6		-4.464	0.845		SAR	2006	2010	4	Tong and others (2013)	
-120.224	35.667		1.856	0.522		SAR	2006	2010	4	Tong and others (2013)	
-120.294	35.738		2.143	0.963		SAR	2006	2010	4	Tong and others (2013)	

Longitude	Latitude	Location	Creep rate (mm/yr)	sig (mm/yr)	Type	Inst	Start	End	Years	Source	Comments
-120.355	35.823		-5.286	3.173		SAR	2006	2010	4	Tong and others (2013)	
-120.418	35.88		14.159	1.672		SAR	2006	2010	4	Tong and others (2013)	
-120.493	35.948		26.732	1.783		SAR	2006	2010	4	Tong and others (2013)	
-120.569	36.011		30.67	3.531		SAR	2006	2010	4	Tong and others (2013)	
-120.645	36.077		26.096	2.101		SAR	2006	2010	4	Tong and others (2013)	
-120.719	36.146		28.821	3.81		SAR	2006	2010	4	Tong and others (2013)	
-120.79	36.206		19.429	3.77		SAR	2006	2010	4	Tong and others (2013)	
-120.862	36.28		24.352	1.965		SAR	2006	2010	4	Tong and others (2013)	
-120.935	36.346		18.891	1.152		SAR	2006	2010	4	Tong and others (2013)	
-121.006	36.419		20.71	3.553		SAR	2006	2010	4	Tong and others (2013)	
-121.077	36.489		22.461	2.733		SAR	2006	2010	4	Tong and others (2013)	
-121.149	36.556		23.446	2.106		SAR	2006	2010	4	Tong and others (2013)	
-121.223	36.623		11.006	1.55		SAR	2006	2010	4	Tong and others (2013)	
-121.301	36.689		7.194	3.438		SAR	2006	2010	4	Tong and others (2013)	
-121.384	36.748		15.479	1.59		SAR	2006	2010	4	Tong and others (2013)	
-121.471	36.802		10.286	1.826		SAR	2006	2010	4	Tong and others (2013)	
-121.557	36.862		4.543	2.084		SAR	2006	2010	4	Tong and others (2013)	
-121.642	36.919		2.192	0.524		SAR	2006	2010	4	Tong and others (2013)	
-121.724	36.981		0.343	1.174		SAR	2006	2010	4	Tong and others (2013)	
-121.891	37.098		-1.91	1.456		SAR	2006	2010	4	Tong and others (2013)	
-121.975	37.16		-4.693	2.182		SAR	2006	2010	4	Tong and others (2013)	
-122.206	37.357		-2.632	3.124		SAR	2006	2010	4	Tong and others (2013)	
-122.342	37.5		-3.671	5.213		SAR	2006	2010	4	Tong and others (2013)	
-122.651	37.877		3.793	3.884		SAR	2006	2010	4	Tong and others (2013)	
-122.715	37.951		-1.183	2.809		SAR	2006	2010	4	Tong and others (2013)	
-122.846	38.098		9.042	5.003		SAR	2006	2010	4	Tong and others (2013)	
-123.041	38.319		0.751	2.882		SAR	2006	2010	4	Tong and others (2013)	
-123.25	38.532		1.216	2.051		SAR	2006	2010	4	Tong and others (2013)	
-123.322	38.603		-4.39	1.316		SAR	2006	2010	4	Tong and others (2013)	
-123.392	38.673		-8.293	3.702		SAR	2006	2010	4	Tong and others (2013)	
-123.462	38.743		-8.131	2.212		SAR	2006	2010	4	Tong and others (2013)	
-123.53	38.817		0.242	1.453		SAR	2006	2010	4	Tong and others (2013)	
-123.596	38.892		-1.14	2.282		SAR	2006	2010	4	Tong and others (2013)	
-123.661	38.965		-3.385	3.239		SAR	2006	2010	4	Tong and others (2013)	
-123.69059	38.99986	Alder Creek	0.4	0.05					29.6	McFarland and others (2011)	
-121.58611	36.88261	Cannon Road	0.1	0.11					8.2	McFarland and others (2011)	
-122.46564	37.64419	Duhallow Way	-0.3	0.02					29.9	McFarland and others (2011)	
-121.52171	36.83502	Mission Vineyard Rd	11.7	0.12					20.1	McFarland and others (2011)	
-122.26154	37.417	Roberta Drive	0.6	0.04					20.5	McFarland and others (2011)	

Longitude	Latitude	Location	Creep rate (mm/yr)	sig (mm/yr)	Type	Inst	Start	End	Years	Source	Comments
-121.5728	36.87453	Searle Rd	1.3	0.26					7.9	McFarland and others (2011)	
-121.185	36.595	Willow Creek	20.2			AA	1967	2004	37	Titus and others (2006)	
-120.9693	36.3833	Smith Ranch	26.2			AA	1970	2003	33	Titus and others (2006)	
-120.9017	36.3167	DeAlvarez Ranch	24			AA	1970	2004	34	Titus and others (2006)	
-120.7983	36.2133	Monarch Peak	17.4			AA	1968	2004	36	Titus and others (2006)	
-120.7567	36.18	Mee Ranch	23.7			AA	1970	2003	33	Titus and others (2006)	
-120.7567	36.18	Mee Ranch	23			AA	1970	2004	34	Titus and others (2006)	
-120.6283	36.065	Slack Canyon	21.2			AA	1968	2003	35	Titus and others (2006)	
-120.6283	36.065	Slack Canyon	23			AA	1968	2004	36	Titus and others (2006)	
-120.4217	35.885	Durham Ranch	8.7			AA	1968	2004	36	Titus and others (2006)	
-120.4217	35.885	Durham Ranch	13.3			AA	1968	2004	36	Titus and others (2006)	
-121.2	36.6	Melendy Ranch	17.6			CM	1969	2004	35	Titus and others (2006)	40 km along fault from creepmeter XSJ2 in San Juan Bautista
-120.6283	36.065	Slack Canyon	20.8			CM	1969	2004	35	Titus and others (2006)	117 km along fault from creepmeter XSJ2 in San Juan Bautista
-120.4	35.8	Taylor Ranch	9.3			CM	1985	2004	19	Titus and others (2006)	144 km along fault from creepmeter XSJ2 in San Juan Bautista
San Gregorio											
-122.4956	37.5038	Seal Cove	-0.2	0.04	Int	AA	1979	2009	30	McFarland and others (2011)	Pre-Loma Prieta rate
-122.3719	37.2546	Pescadero	1	0.07	Int	AA	1982	2009	27	McFarland and others (2011)	Pre-Loma Prieta rate
San Jacinto											
-117.264	34.0442	Claremont (Colton)	0	1	Int	AA	1973	1983		Louie and others (1985)	
-116.669	33.5861	Clark (Anza)	0	2	Int	AA	1977	1984		Louie and others (1985)	
-116.05	33.09	Coyote Creek (BW)	5.2	3	Int+Aft	AA	1971	1984		Louie and others (1985)	accelerated by 1968 EQ
-116.004	33.033		-1.629	1.614		SAR	2006	2010		Tong and others (2013)	
-116.056	33.099		8.579	0.896		SAR	2006	2010		Tong and others (2013)	
-116.143	33.164		2.212	1.18		SAR	2006	2010		Tong and others (2013)	
-116.217	33.222		0.186	0.398		SAR	2006	2010		Tong and others (2013)	
-116.296	33.282		-2.118	0.745		SAR	2006	2010		Tong and others (2013)	
-116.371	33.346		-0.184	0.806		SAR	2006	2010		Tong and others (2013)	
-116.453	33.407		-0.659	0.26		SAR	2006	2010		Tong and others (2013)	
-116.516	33.473		-1.115	0.675		SAR	2006	2010		Tong and others (2013)	
-116.588	33.538		0.709	0.569		SAR	2006	2010		Tong and others (2013)	
-116.679	33.594		0.317	1.258		SAR	2006	2010		Tong and others (2013)	
-116.763	33.647		1.189	1.053		SAR	2006	2010		Tong and others (2013)	
-116.855	33.698		0.806	1.565		SAR	2006	2010		Tong and others (2013)	
-116.952	33.753		2.23	1.063		SAR	2006	2010		Tong and others (2013)	

Longitude	Latitude	Location	Creep rate (mm/yr)	sig (mm/yr)	Type	Inst	Start	End	Years	Source	Comments
-116.966	33.815		-12.948	2.936		SAR	2006	2010		Tong and others (2013)	
-117.055	33.877		0.362	3.404		SAR	2006	2010		Tong and others (2013)	
-117.135	33.938		-5.653	1.462		SAR	2006	2010		Tong and others (2013)	
-117.215	34.001		1.442	0.678		SAR	2006	2010		Tong and others (2013)	
-117.287	34.067		0.61	0.69		SAR	2006	2010		Tong and others (2013)	
-117.358	34.135		6.505	2.733		SAR	2006	2010		Tong and others (2013)	
-117.424	34.198		-0.316	2.192		SAR	2006	2010		Tong and others (2013)	
-117.518	34.253		-0.875	2.281		SAR	2006	2010		Tong and others (2013)	
-117.602	34.311		-0.308	1.204		SAR	2006	2010		Tong and others (2013)	
Bartlett Springs											
-122.9526	39.4539	Bartlett Spgs	8.2	2	Int	Model	1991	1995	4	Freymueller and others (1999)	unconfirmed
-122.532	39.038	Bartlett Spgs	0.517	0.962		SAR	2006	2010	4	Tong and others (2013)	
-122.623	39.107	Bartlett Spgs	1.776	1.369		SAR	2006	2010	4	Tong and others (2013)	
-122.692	39.17	Bartlett Spgs	-4.98	2.055		SAR	2006	2010	4	Tong and others (2013)	
-122.768	39.234	Bartlett Spgs	0.268	0.93		SAR	2006	2010	4	Tong and others (2013)	
-122.833	39.304	Bartlett Spgs	-0.428	1.171		SAR	2006	2010	4	Tong and others (2013)	
-122.899	39.378	Bartlett Spgs	-2.381	1.95		SAR	2006	2010	4	Tong and others (2013)	
-122.959	39.454	Bartlett Spgs	-0.123	2.04		SAR	2006	2010	4	Tong and others (2013)	
-123.02	39.533	Bartlett Spgs	6.946	4.026		SAR	2006	2010	4	Tong and others (2013)	
-123.24764	39.75873	Fairbanks Rd	0.9	Unknown					1	McFarland and others (2011)	
-122.95726	39.4456	Lake Pillsbury	3.1	0.32					4.8	McFarland and others (2011)	
-122.71436	39.1938	Newman Spgs	0	1.1					2	McFarland and others (2011)	
-123.22755	39.74003	Round Valley	-0.2	0.6					2	McFarland and others (2011)	
Green Valley											
-122.1495	38.1986	GV	4.4	0.1	Int	AA	1984	2001	17	Galehouse and Lienkaemper (2003)	
-122.117	38.119	Green Valley	2.505	12.888		SAR	2006	2010	4	Tong and others (2013)	
-122.151	38.207	Green Valley	8.244	9.109		SAR	2006	2010	4	Tong and others (2013)	
-122.179	38.294	Green Valley	18.712	18.421		SAR	2006	2010	4	Tong and others (2013)	
-122.24806	38.47626	Crystal Lake	3.1	3.8					3.3	McFarland and others (2011)	
-122.1556	38.21861	Dynasty Court	3.2	Unknown					0.9	McFarland and others (2011)	
-122.16186	38.23603	Mason Rd	0.4	0.53					5.8	McFarland and others (2011)	
-122.11316	38.11413	Parish Rd	3.3	0.6					3.4	McFarland and others (2011)	
-122.15054	38.19848	Red Top Rd	3.7	0.08					25.9	McFarland and others (2011)	
-122.1368	38.16584	S Ridgefield Way	8.8	Unknown					0.9	McFarland and others (2011)	

Longitude	Latitude	Location	Creep rate (mm/yr)	sig (mm/yr)	Type	Inst	Start	End	Years	Source	Comments
Superstition Hills											
-115.6633	32.9045	Superstition Hills	0.5	Undefined	Int	CM	1968	1979		Louie and others (1985)	
-115.692	32.923	Superstition	1.066	2.93		SAR	2006	2010		Tong and others (2013)	
-115.769	32.984	Superstition	2.786	0.4		SAR	2006	2010		Tong and others (2013)	
Greenville											
-121.69817	37.7206	Altamont Pass Rd	2.1	Unknown					1.2	McFarland and others (2011)	
		Main	1.06	0.21							
		West	0.55	0.11							
Hunting Creek											
-122.38873	38.81388	Hunting Creek	1.8	0.8					3.1	McFarland and others (2011)	
Saltillo and Cerro Prieto											
32.426389	-115.128	Saltillo	5.3-7.3							Glowacka and others (2010)	
32.420556	115.1281	Saltillo		2						Glowacka and others (2010)	Instrument rotated; actual horizontal creep may be lower.
32.354444	-115.231	Cerro Prieto	1.3							Glowacka and others (2010)	

Table D3. Creep rates from repeating earthquakes.

[Data from Templeton and others, 2008; creep rate (last column) calculated here is average slip per event/average time between slip events. Burst events and events outside area of interest are not included. avg, average; mm, millimeters; mm/yr, millimeters per year]

Sequence label number	Latitude (avg)	Longitude (avg)	Sequence depth (avg)	Median sequence magnitude	Total slip (mm)	Creep rate (mm/yr)
33	36.8242	-121.5483	6.30	2.69	423	20.0
32	36.8238	-121.5462	5.88	2.09	372	17.6
31	36.8248	-121.5437	4.30	1.91	268	12.7
34	36.8194	-121.5362	5.23	2.65	414	19.5
35	36.8192	-121.5338	4.48	1.58	276	13.0
130	36.8036	-121.5311	8.30	1.49	52	2.4
36	36.8119	-121.5311	6.59	1.59	277	13.1
38	36.8112	-121.5286	5.57	2.39	266	12.6
37	36.8125	-121.5285	5.15	2.14	153	7.2
40	36.8102	-121.5265	5.31	1.51	265	12.5
41	36.8041	-121.5264	7.35	2.12	379	17.9
43	36.7990	-121.5240	7.34	2.49	188	8.9
39	36.8117	-121.5229	4.93	2.55	98	4.6
44	36.7985	-121.5204	7.05	2.23	323	15.3
42	36.8074	-121.5199	3.89	1.62	113	5.3
131	36.7896	-121.5145	8.72	1.75	61	2.8
45	36.7983	-121.5094	6.67	1.25	273	12.9
132	36.7911	-121.5034	6.92	1.47	52	2.4
133	36.7912	-121.5010	6.05	1.33	48	2.2
134	36.7867	-121.5000	6.51	1.88	66	3.0
135	36.7883	-121.4983	6.34	1.44	152	7.0
136	36.7832	-121.4975	6.69	1.77	62	2.8
46	36.7822	-121.4809	4.38	1.74	242	11.5
137	36.7683	-121.4805	7.65	1.48	52	2.4
138	36.7658	-121.4783	8.31	1.70	178	8.1
48	36.7738	-121.4744	6.46	1.58	55	2.6
51	36.7711	-121.4742	7.22	1.63	170	8.1
50	36.7702	-121.4741	6.89	2.02	143	6.8
49	36.7689	-121.4740	6.49	2.19	79	3.7
47	36.7748	-121.4719	4.73	2.85	465	22.0
139	36.7613	-121.4714	8.34	1.46	154	7.1
52	36.7731	-121.4699	7.06	1.22	179	8.4
140	36.7620	-121.4697	8.94	1.56	55	2.6
53	36.7680	-121.4666	7.04	1.65	172	8.1
54	36.7627	-121.4642	6.94	2.98	126	5.9
144	36.7391	-121.4641	15.17	1.60	56	2.6
58	36.7487	-121.4602	9.44	2.58	199	9.1

Sequence label number	Latitude (avg)	Longitude (avg)	Sequence depth (avg)	Median sequence magnitude	Total slip (mm)	Creep rate (mm/yr)
55	36.7662	-121.4578	4.92	2.27	248	11.7
141	36.7606	-121.4570	6.53	2.08	74	3.5
56	36.7609	-121.4567	6.50	2.20	159	7.3
57	36.7498	-121.4537	8.82	1.65	287	13.2
61	36.7488	-121.4469	8.03	2.48	187	8.6
59	36.7533	-121.4444	6.10	2.09	298	13.6
142	36.7488	-121.4417	7.58	1.92	67	3.2
60	36.7538	-121.4394	6.71	1.87	196	9.0
143	36.7487	-121.4363	6.45	1.87	65	3.1
62	36.7449	-121.4317	6.34	2.21	319	14.6
14	36.9054	-121.4226	3.88	1.60	112	5.3
19	36.8580	-121.4168	4.29	1.51	53	2.5
63	36.7400	-121.4166	6.85	1.58	221	10.1
15	36.8848	-121.4156	7.36	1.82	127	6.0
16	36.8837	-121.4144	7.71	2.07	74	3.5
17	36.8777	-121.4142	7.90	1.42	100	4.7
18	36.8768	-121.4137	7.11	1.88	132	6.2
64	36.7401	-121.4106	6.77	1.79	125	5.7
20	36.8372	-121.4093	8.44	2.09	74	3.5
21	36.8301	-121.4082	8.23	1.34	48	2.3
22	36.8305	-121.4078	8.51	1.55	108	5.1
25	36.7858	-121.4076	8.67	1.46	51	2.4
65	36.7360	-121.4051	6.95	1.96	207	9.5
67	36.7356	-121.4030	6.89	1.78	310	14.2
66	36.7350	-121.4026	6.33	2.38	265	12.1
23	36.8042	-121.3900	6.14	1.29	140	6.6
24	36.8010	-121.3882	6.76	2.14	77	3.6
68	36.7329	-121.3867	2.91	1.85	194	8.9
69	36.7234	-121.3680	2.80	2.08	370	16.9
70	36.7226	-121.3674	2.98	1.84	514	23.6
71	36.7207	-121.3638	2.97	2.14	307	14.0
73	36.7139	-121.3577	2.67	1.91	469	21.5
145	36.7195	-121.3571	5.92	1.39	49	2.3
72	36.7145	-121.3560	2.96	2.21	479	21.9
74	36.7142	-121.3558	3.08	1.90	399	18.3
76	36.7120	-121.3477	1.33	2.11	75	3.4
1	36.8822	-121.3462	6.21	1.39	49	2.3
77	36.7082	-121.3458	2.95	1.73	422	19.3
75	36.7127	-121.3457	1.51	2.27	414	18.9
78	36.7031	-121.3383	4.73	2.17	390	17.9
146	36.6994	-121.3368	4.61	1.72	60	2.7

Sequence label number	Latitude (avg)	Longitude (avg)	Sequence depth (avg)	Median sequence magnitude	Total slip (mm)	Creep rate (mm/yr)
79	36.7045	-121.3354	2.96	2.35	87	4.0
81	36.6992	-121.3326	4.07	2.27	165	7.6
80	36.6994	-121.3314	2.97	2.06	292	13.4
82	36.6942	-121.3248	4.78	2.47	93	4.3
83	36.6930	-121.3244	4.67	1.95	343	15.7
84	36.6932	-121.3240	3.85	1.84	450	20.6
87	36.6859	-121.3172	5.97	1.68	176	8.0
86	36.6882	-121.3171	4.40	1.85	582	26.7
85	36.6890	-121.3171	4.23	2.23	242	11.1
2	36.8508	-121.3144	5.67	1.96	69	3.3
88	36.6852	-121.3143	5.52	1.84	257	11.8
89	36.6857	-121.3137	4.28	1.85	452	20.7
147	36.6789	-121.3097	5.81	1.47	52	2.4
90	36.6837	-121.3083	4.01	2.05	145	6.7
91	36.6827	-121.3075	3.89	2.05	291	13.3
92	36.6802	-121.3065	2.78	2.04	144	6.6
148	36.6767	-121.3052	5.89	1.67	58	2.7
149	36.6774	-121.3048	6.40	2.77	111	5.1
150	36.6766	-121.3045	5.35	1.69	59	2.7
93	36.6788	-121.3039	5.38	2.47	93	4.3
3	36.8401	-121.3019	4.29	2.33	86	4.0
5	36.8375	-121.3014	4.09	1.71	119	5.6
4	36.8396	-121.3014	4.32	2.27	165	7.8
94	36.6769	-121.2996	3.00	2.19	237	10.8
95	36.6746	-121.2967	3.85	1.81	316	14.5
96	36.6745	-121.2966	4.34	2.34	86	3.9
6	36.8336	-121.2963	4.09	1.60	56	2.6
97	36.6741	-121.2959	3.93	2.28	333	15.2
7	36.8327	-121.2949	3.65	1.39	148	7.0
8	36.8310	-121.2903	6.03	2.01	71	3.4
98	36.6687	-121.2870	3.04	2.69	212	9.7
101	36.6655	-121.2869	5.85	2.15	154	7.1
100	36.6663	-121.2869	2.92	2.32	170	7.8
99	36.6683	-121.2860	3.25	3.07	397	18.2
10	36.7715	-121.2859	8.05	1.37	98	4.6
103	36.6594	-121.2858	7.66	2.79	112	5.1
9	36.7770	-121.2855	9.24	1.78	248	11.7
102	36.6616	-121.2846	6.53	2.96	124	5.7
26	36.6894	-121.2828	4.66	1.53	107	5.1
108	36.6564	-121.2818	8.36	2.91	241	11.0
27	36.6872	-121.2814	4.55	1.65	58	2.7

Sequence label number	Latitude (avg)	Longitude (avg)	Sequence depth (avg)	Median sequence magnitude	Total slip (mm)	Creep rate (mm/yr)
109	36.6550	-121.2807	7.52	2.50	189	8.7
28	36.6863	-121.2803	5.14	1.53	54	2.5
110	36.6543	-121.2801	7.74	2.56	98	4.5
111	36.6535	-121.2781	7.53	2.20	159	7.3
104	36.6604	-121.2771	3.41	3.17	421	19.3
112	36.6529	-121.2770	7.47	2.27	248	11.4
29	36.6812	-121.2764	5.17	1.72	60	2.8
105	36.6578	-121.2752	3.34	2.38	265	12.1
106	36.6563	-121.2749	5.57	2.64	308	14.1
113	36.6527	-121.2742	6.58	2.43	364	16.7
114	36.6521	-121.2733	6.80	2.16	155	7.1
11	36.7598	-121.2732	7.88	1.67	233	11.0
115	36.6507	-121.2721	6.61	2.23	323	14.8
107	36.6570	-121.2716	3.47	2.73	108	5.0
116	36.6506	-121.2710	6.73	2.55	390	17.9
117	36.6530	-121.2700	3.34	2.04	144	6.6
118	36.6514	-121.2683	5.13	2.55	390	17.9
121	36.6458	-121.2677	7.29	2.54	194	8.9
120	36.6492	-121.2664	5.50	2.06	292	13.4
119	36.6515	-121.2649	3.72	3.07	265	12.1
122	36.6431	-121.2647	8.56	2.49	94	4.3
30	36.6706	-121.2633	4.33	1.65	58	2.7
125	36.6422	-121.2609	7.12	2.52	96	4.4
124	36.6440	-121.2595	5.74	2.01	213	9.8
123	36.6452	-121.2585	4.61	2.23	404	18.5
12	36.7552	-121.2575	9.95	1.59	222	10.5
126	36.6425	-121.2569	5.69	2.57	296	13.6
128	36.6422	-121.2554	4.50	2.19	395	18.1
127	36.6432	-121.2548	3.95	2.48	187	8.6
129	36.6411	-121.2542	5.58	2.77	111	5.1
13	36.7390	-121.2042	9.57	1.44	102	4.8